Stockholm University

Transition metal-catalyzed reduction of carbonyl compounds

Fe, Ru and Rh complexes as powerful hydride mediators

Elina Buitrago

ISBN 978-91-7447-506-7

Printed in Sweden by US-AB, Stockholm 2012
Distributor: Department of Organic Chemistry, Stockholm University

Abstract

A detailed mechanistic investigation of the previously reported ruthenium pseudo-dipeptide-catalyzed asymmetric transfer hydrogenation (ATH) of aromatic ketones was performed. It was found that the addition of alkali metals has a large influence on both the reaction rate and the selectivity, and that the rate of the reaction was substantially increased when THF was used as a co-solvent. A novel bimetallic mechanism for the ruthenium pseudo-dipeptide-catalyzed asymmetric reduction of prochiral ketones was proposed.

There is a demand for a larger substrate scope in the ATH reaction, and heteroaromatic ketones are traditionally more challenging substrates. Normally a catalyst is developed for one benchmark substrate, and a substrate screen is carried out with the best performing catalyst. There is a high probability that for different substrates, another catalyst could outperform the one used. To circumvent this issue, a multiple screen was executed, employing a variety of ligands from different families within our group's ligand library, and different heteroaromatic ketones to fine-tune and to find the optimum catalyst depending on the substrate. The acquired information was used in the formal total syntheses of (*R*)-fluoxetine and (*S*)-duloxetine, where the key reduction step was performed with high enantioselectivities and high yield, in each case.

Furthermore, a new iron-*N*-heterocyclic carbene (NHC)-catalyzed hydrosilylation (HS) protocol was developed. An active catalyst was formed *in situ* from readily available imidazolium salts together with an iron source, and the inexpensive and benign polymethylhydrosiloxane (PMHS) was used as hydride donor. A set of sterically less demanding, potentially bidentate NHC precursors was prepared. The effect proved to be remarkable, and an unprecedented activity was observed when combining them with iron. The same system was also explored in the reduction of amides to amines with satisfactory results.

List of publications

This thesis is based on the following papers, which will be referred to by Roman numerals. Reprints were produced with the kind permission of the publisher.

I. **Mechanistic Investigations into the Asymmetric Transfer Hydrogenation of Ketones Catalyzed by Pseudo-dipeptide Ruthenium Complexes**
Wettergren, J.; Buitrago, E.; Ryberg, P.; Adolfsson, H.
Chem. Eur. J. **2009**, *15*, 5709 – 5718

II. **High throughput screening of a catalyst library for asymmetric transfer hydrogenation of heteroaromatic ketones. Formal syntheses of (*R*)-fluoxetine and (*S*)-duloxetine.**
Buitrago, E.; Lundberg, H.; Andersson, H. G.; Ryberg, P.; Adolfsson, H
Manuscript

III. **Selective hydrosilylation of ketones by *in situ* generated iron NHC complexes**
Buitrago, E.; Zani, L.; Adolfsson, H.
Appl. Organomet. Chem. **2011**, *25*, 748 – 752

IV. **Efficient and Selective Hydrosilylation of Carbonyls Catalyzed by Iron Acetate and *N*-Hydroxyethylimidazolium Salts**
Buitrago, E.; Tinnis, F.; Adolfsson, H.
Adv. Synth. Catal. **2012**, *354*, 217 – 222

Appendix B **Direct hydrosilylation of tertiary amides to amines in an efficient iron-NHC-catalyzed procedure**
Buitrago, E.; Volkov, A.; Adolfsson, H.

Contents

Abbreviations

Abbreviations and acronyms are used in agreement with the standard of the subject. Only nonstandard and unconventional ones that appear in the thesis are listed here.

ATH	Asymmetric transfer hydrogenation
BDSB	*p*-bis(dimethylsilyl)benzene
CBS	Corey-Bakshi-Shibata
DIOP	2,2-dimethyl-4,5-bis(diphenylphosphinomethyl)-1,3-dioxolane
DKR	Dynamic kinetic resolution
DMHEMIM	Dimethoxyhydroxyethylimidazole
DMIM	Dimethylimidazole
dppb	Diphenylphosphinobutane
ee	Enantiomeric excess
HEMIM	Hydroxyethylimidazole
HMB	Hexamethyl benzene
HS	Hydrosilylation
KIE	Kinetic isotope effect
KR	Kinetic resolution
MPV	Meerwein-Ponndorf-Verley
NHC	*N*-heterocyclic carbene
NMM	*N*-methyl morpholine
PCA	Principal component analysis
PMHS	Polymethylhydrosiloxane
SSRI	Selective Serotonin Reuptake Inhibitors
S,*S*-Me-Duphos	(+)-1,2-Bis[(2*S*,5*S*)-2,5-dimethylphospholano]benzene
TEAF	Triethyl ammonium formate
TH	Transfer hydrogenation
TMDS	Tetramethyldisiloxane
TsDPEN	(1*S*,2*S*)-(+)-*N*-*p*-Tosyl-1,2-diphenylethylene diamine

x

1. Introduction

Secondary alcohols are important building blocks for the synthesis of a number of pharmaceuticals, agrochemicals and fine chemicals. The reduction of carbonyl compounds to yield secondary alcohols is a very desirable reaction, since carbonyl compounds are among the most abundant starting materials for a synthetic chemist. The reduction of a prochiral ketone results in the formation of a chiral compound.

A molecule is said to be chiral when the two mirror images are non-superimposable on each other. The two molecular mirror images are called enantiomers. In a symmetric environment the two enantiomers have the same physical and chemical properties, except for the rotation of plane-polarized light. In a chiral environment, however, the two enantiomers can behave rather differently. Enantiomerically enriched compounds refer to samples having a higher content of one of the two enantiomers.

Single enantiomer drugs are of great importance in the cases where the two enantiomers affect the body in different ways, and the number of single enantiomer drugs is constantly increasing. One example is the asthma medication albuterol (Figure 1), a secondary alcohol where the *R*-isomer has the desired effect of widening the airways, while the *S*-isomer increases the patients' reactivity to stimuli, which leads to a more severe asthma attack.[1]

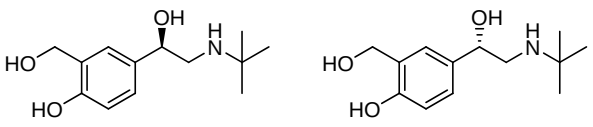

(*R*)-albuterol (*S*)-albuterol

Figure 1 *R* and *S* enantiomers of albuterol, Ventoline ™

There are several different methods available to obtain enantioenriched compounds. One is to start with materials from the chiral pool, naturally occurring enantiopure compounds, such as sugars or amino acids, and maintain the enantiopurity intact throughout the synthesis. These compounds often have a high availability, low cost and high enantiomerical purity, however, the method is limited by the fact that in general only one of the enantiomers is naturally occurring.

It is also possible to start from a mixture of the two enantiomers, a racemate, and separate them by converting them into the corresponding diastereomers by addition of a resolving agent. The diastereomers have different physical properties, and can be separated. Kinetic resolution is a variant where a chiral catalyst (organocatalyst, enzyme, metal catalyst) reacts with one of the enantiomers rapidly, and leaves the other one unreacted. The limitation with kinetic resolution is that the maximum yield for the reaction is 50%, but despite this drawback, it is the most commonly used method in industry.[2] To circumvent this limitation, a racemization catalyst can be added to the reaction, increasing the maximum yield to 100%, in a process termed dynamic kinetic resolution.[3]

Another approach is to use asymmetric synthesis. The stereochemical outcome in such a process is determined by the substrate, a reagent or a chiral catalyst. The use of a chiral catalyst is most advantageous, since only a small amount of enantiopure material is needed. Precious metal catalysts are the most commonly used for these transformations, due to their high activities, large substrate scopes, and because in many cases the reactivity and enantioselectivity can be tuned by altering the ancillary ligands. Lately, effort has been put into the development of the area of green catalysis. There is considerable interest in replacing the commonly used precious metals, due to their inherent toxicity and their high cost, with more cost effective and environmentally benign alternatives. Other green approaches are to use lower catalyst loadings, greener reaction media and milder reaction conditions. There are also numerous organocatalytic methods for obtaining enantioenriched compounds, where small, chiral organic molecules catalyze a reaction with stereochemical induction.[4]

1.1 Reductions

There is an immense variety of different reduction protocols that have been developed for unsaturated compounds, however, this thesis will only focus on the reduction of carbonyl compounds. The latter reductions are traditionally performed using stoichiometric amounts of hydride reagents, such as $LiAlH_4$ or $NaBH_4$, which are highly reactive and sometimes difficult to handle. Asymmetric catalytic reduction is often used to obtain enantiomerically enriched alcohols from prochiral ketones, using a transition metal catalyst in combination with molecular hydrogen (hydrogenation),[5] or formic acid/2-propanol (transfer hydrogenation).[6] An alternative method is the catalytic two-step process involving hydrosilylation followed by hydrolysis of the resulting silyl-ether. In this thesis the focus is on the latter two methods, transfer hydrogenation and hydrosilylation.

1.2 Transition metal-catalyzed transfer hydrogenation

1.2.1 The transfer hydrogenation reaction

Transfer hydrogenation is defined as "reduction of multiple bonds with the aid of a hydrogen donor in presence of a catalyst".[6b] The reaction was discovered in the 1920s by Meerwein, Verley and Ponndorf,[7] where aluminum isopropoxide was used to promote the transfer of hydrogen from isopropoxide to a ketone, forming the corresponding secondary alcohol along with acetone. The hydride is transferred via a six-membered transition state, in which the ketone and 2-propanol are simultaneously coordinated to the aluminum ion, which enables the hydride transfer (Scheme 1). The reaction is reversible and an excess of 2-propanol is used to drive the reaction toward the reduction of the ketone, whereas the presence of an excess of acetone leads to oxidation of alcohols. The reverse process was studied by Oppenauer in 1937 and is referred to as the Oppenauer oxidation.[8]

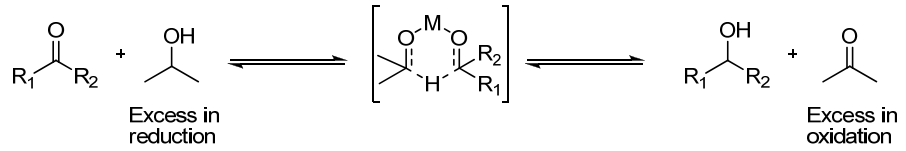

Scheme 1 Meerwein-Ponndorf-Verley reduction and Oppenauer oxidation.

The first transition metal-catalyzed transfer hydrogenation was reported in the 1960's.[9] In the 1970s is was discovered that $[Ru(PPh_3)Cl_2]$ had catalytic activity at high temperatures, although the reaction was very slow.[10] In 1991, Bäckvall and Chowdhury reported that adding a small amount of base as a catalyst promoter increased the reaction rate dramatically.[11] The effect of the base was ascribed to the formation of an isopropoxide ion, which can coordinate to ruthenium to facilitate the formation of a metal hydride through a β-elimination. The most widely used hydrogen donors for the transfer hydrogenation are 2-propanol, and a 5:2 mixture of formic acid and triethylamine, which forms an azeotrope (triethyl ammonium formate, TEAF, in formic acid). Using the hydrogen donor as reaction medium allows for a large excess of the hydrogen donor, which drives the equilibrium toward the reduction of the ketone. There are also examples of greener approaches using water as the reaction medium, with sodium formate as the hydrogen source.[12] Using TEAF or sodium formate irreversibly forms carbon dioxide upon reaction, which favors the required reaction, but typically the reaction is faster using 2-propanol.

1.2.2 Mechanistic aspects

There are two general pathways for the hydride transfer in the transfer hydrogenation reaction: direct hydrogen transfer and the hydridic route.[13] The direct hydrogen transfer is a concerted process in which the donor and the acceptor are both coordinated to the metal, and the hydride is transferred from the alkoxide to the ketone in a six-membered transition state. The metal acts as a Lewis acid activating the substrate towards the nucleophilic attack of the hydride. The MPV reaction is an example which proceeds via this mechanism (Scheme 1). Direct hydride transfer is typical for main group metals, whereas transition metals often form intermediate metal hydrides.[13] The hydridic route involves formation of a metal hydride by interaction of the catalyst with the hydrogen donor, and this hydride is subsequently transferred to the substrate. The hydridic route is further divided into the monohydridic route and the dihydridic route, depending on the nature of the complex.[6c, 14] In the dihydride mechanism, both the C-H and the O-H from the hydrogen donor end up on the metal, and their identity is lost in this transfer, while in the monohydridic mechanism the C-H hydride of the donor forms the metal hydride, which is in turn transferred to the carbonyl carbon of the substrate.

There are two possible means for the hydride transfer from the catalyst to the substrate in the monohydridic mechanism. The hydride can be transferred in the inner sphere of the metal, involving the formation of a metal alkoxide, or it can occur in the outer sphere of the metal, without coordination of the hydrogen donor to the metal, usually by interaction with a ligand which is coordinated to the metal. The outer sphere mechanism can be a concerted process or can occur in two discrete steps, namely protonation followed by hydride transfer.[13]

Scheme 2 Inner- (a) vs. outer- (b) sphere mechanism.

A catalyst containing both an acidic and a basic site is required for an outer sphere hydrogen transfer, and this class of complexes is referred to as ligand metal bifunctional catalysts.[15] The basic center of the ligand is suggested to interact with the substrate oxygen via a hydrogen bond, and thereby facilitate the hydride transfer. A proton and a hydride can be transferred in a concerted six-membered transition state, without direct coordination of the substrate to the metal center.

1.2.3 The asymmetric transfer hydrogenation reaction

Transfer hydrogenation can be performed in an asymmetric fashion using a chiral catalyst which consists of a metal combined with a chiral ligand. Major progress has been made in this field, and there are a large number of different catalysts reported for the transfer hydrogenation of ketones. Among the most successful catalysts are the ones derived from ligands such as the bidentate 1,2-amino alcohol **1** developed by Andersson in 2001[16] and the dipshosphonite **2** utilised by Reetz[17] (Figure 2).

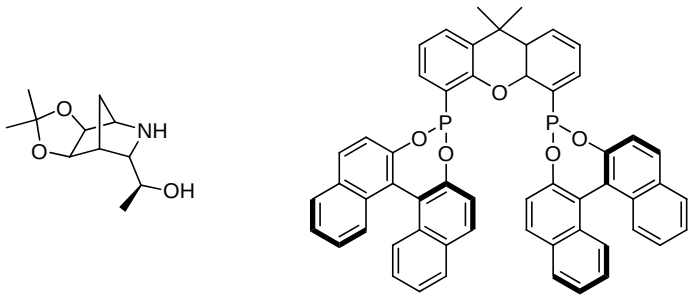

1 **2**

Figure 2 Succesful ligands for the ruthenium-catalyzed ATH of ketones.

Noyori's monotosylated diamine and ruthenium based protocol, published in 1995, is up to today one of the most efficient catalytic systems for ATH of ketones, and it has been studied extensively.[15] In the bifunctional, active catalyst, the enantioselectivity is induced by the chiral ligand, where the basic nitrogen in the ligand works as a proton acceptor and donor, while the metal takes up and delivers the hydride. The high selectivity associated with reduction of aryl ketones, as opposed to dialkyl ketones, is attributed to dipolar interactions between the arene-CH of the catalyst and the π-system of the ketone.[18]

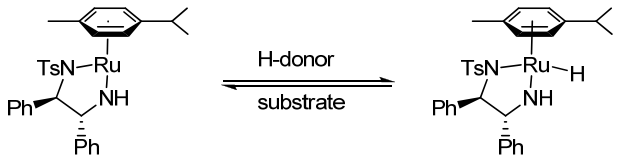

Scheme 3 The Noyori bifunctional catalyst.

In 2005, Baratta reported a pincer type catalyst **3**, which showed exceptional activity in TH,[19] and shortly thereafter he published the asymmetric version **4**. With a catalyst loading of only 0.005%, a TOF value of 1.4 x 10^6 h^{-1} was obtained, although with a moderate *ee* of 88%.[20] Baratta also prepared an osmium complex **5**, that showed similar activity, but with an improved *ee* of 98% (Figure 3).[21]

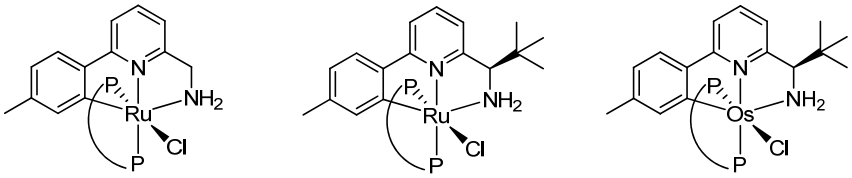

3
PP: dppb

4
PP: dppb

5
PP: (*S*,*R*)-Josiphos

Figure 3 Baratta's ruthenium and osmium pincer complexes for the ATH.

Lately, the use of more inexpensive and environmentally benign metals has been studied intensely, and of those studied, an iron-based catalyst system developed by Morris is the most prominent in terms of activity and selectivity in the ATH reaction.[22]

1.3 Hydrosilylation of carbonyl compounds

1.3.1 The hydrosilylation reaction

The hydrosilylation reaction is described as the addition of Si-H across unsaturated bonds. One of the major advantages of the hydrosilylation procedure compared to other reduction methods is that mild conditions are usually required. Mildly hydridic silanes, which are chemically stable and easy to handle, are used as hydride donors when being activated by a catalyst or an additive. The primary product in the hydrosilylation reaction of ketones or aldehydes is a silyl ether, which can easily be hydrolyzed to the corresponding alcohol. The most common mode of activation of the silane is believed to be oxidative addition of the silyl hydride to a transition metal center.

There are also examples of non-transition metal-catalyzed hydrosilylations. In these cases the most common reaction approach is promotion by Brønsted acids, Lewis acids or Lewis bases. Carbonyl reduction using silanes in Brønsted acidic media is a well-established methodology, and the use of Lewis acids to activate the carbonyl has also been studied. In the Lewis base activation strategy the hydride transfer from the weakly Lewis acidic silicon center is promoted by addition of a nucleophile to the silane. This leads to a hypervalent silicon intermediate which is a potent hydride transfer reagent.[23]

Both phenyl silanes and alkoxysilanes are commonly used monomeric silanes for this type of reaction, the most widely used silane reagents are diphenylsilane, Ph_2SiH_2, and diethoxymethylsilane, $(EtO)_2MeSiH$. These types of silanes are quite sensitive to air and moisture, and need to be handled under inert conditions. Furthermore, the price of such silanes is relatively high. Polymethylhydrosiloxane (PMHS) is an attractive reducing agent for the hydrosilylation reaction due to its low cost, low toxicity and high stability. PMHS air and moisture stable, and the lack of reactivity in the absence of a catalyst makes it easy to handle.[24]

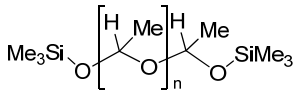

Figure 4 Polymeric hydrosilane PMHS.

1.3.2 Transition metal-catalyzed asymmetric hydrosilylation

Transition metal-catalyzed hydrosilylation is a highly developed field of carbonyl reductions, with rhodium catalysts being the most prevalent. Hydrosilylation is similar to hydrogenation, with a hydrosilane as the hydride donor instead of molecular hydrogen, and similar catalysts are often used. Wilkinson's rhodium complex $RhCl(PPh_3)_3$, was employed in 1973 by Corriu and co-workers as one of the first catalysts for hydrosilylation of carbonyl compounds.[25] The first report of the asymmetric hydrosilylation of ketones and imines came from Kagan and co-workers, who used a rhodium DIOP catalyst.[26]

Catalytic hydrosilylation has been extensively studied since then, and numerous rhodium and titanium-catalyzed systems for the asymmetric hydrosilylation of ketones have been reported.[27] A variety of ligands and silanes have been used, and a wide range of ketones can be reduced in moderate to high enantioselectivity.[28] Early results indicated that nitrogen-based ligands together with rhodium could give high enantioselectivities, which inspired the development of a variety of P,N-ligands. Some of the most successful ligands are the bis(oxazoline)pyridine Pybox **6**,[29] the phosphinooxazolines **7** developed by Helmchen[30] and Williams[31] and the pyridine ferrocene containing ligand **8** developed by Fu and Tao (Figure 5).[32]

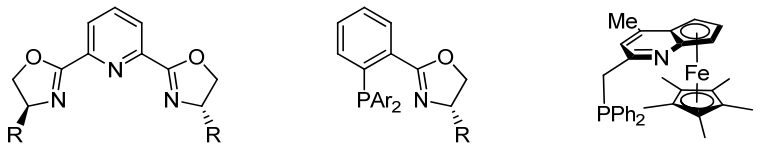

6 **7** **8**

Figure 5 Pybox, phosphinooxazoline and pyridine ferrocene ligands for Rh-catalyzed asymmetric hydrosilylation.

In the early 1990's the use of titanocene-based chiral catalysts together with PMHS was discovered by Buchwald,[33] Halterman[34] and Harrod.[35] There are also examples of titanium complexes with BINOL[36] and bis(oxazolines),[37] in which the reaction proceeds via a titanium(IV) hydride.

One of the major breakthroughs in the field of asymmetric hydrosilylation was the discovery of chiral zinc catalysts using PMHS as hydride donor.[38] There are several examples of zinc-catalyzed hydrosilylations, and considerable effort has been put into replacing expensive and relatively toxic transition metals with more benign alternatives, for example copper,[39] and in particular iron (*vide infra*).

In cases involving transition metals, the Si-H bond is activated by interaction with the metal center. A mechanism for the hydrosilylation catalyzed by group 8 – 10 transition metals was postulated by Ojima and co-workers in 1972,[40] and it was later verified for the rhodium-catalyzed asymmetric hydrosilylation in 1976.[41] The first step is the oxidative addition of the metal into the Si-H bond, which leads to intermediate II (Scheme 4). The resulting intermediate II then undergoes a ligand exchange to coordinate the carbonyl donor, which is followed by silylmetalation to IV. The silyl ether product is then released in a final reductive elimination step.[23]

Early transition metals and group 11 and 12 transition metals are not prone to oxidatively add into the Si-H bond. Instead a sigma bond metathesis is envisioned and a metal hydride is formed, which is transferred to the electrophilic carbon upon coordination of the carbonyl to the metal.[23]

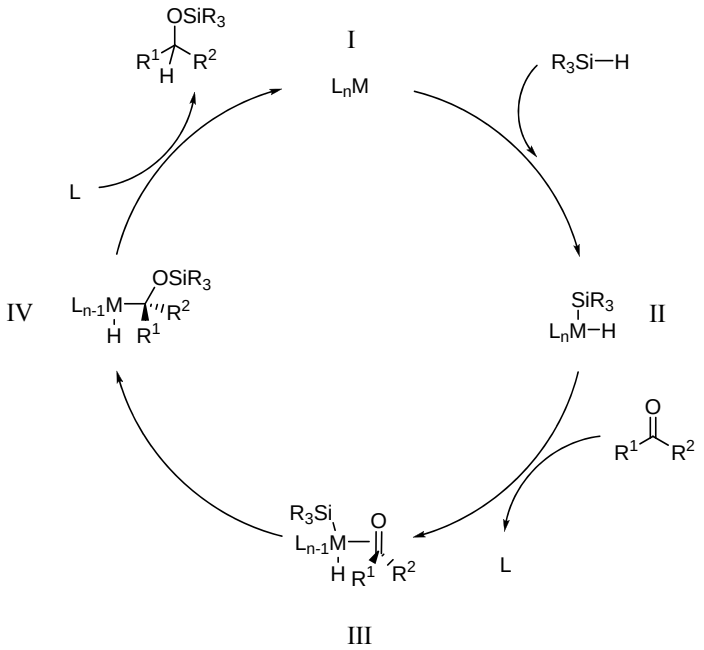

Scheme 4 The generally accepted mechanism for the transition metal-catalyzed hydrosilylation of ketones.

2. Mechanistic studies on the asymmetric transfer hydrogenation of ketones catalyzed by pseudo-dipeptide ruthenium complexes (Paper I)

In our research group we have focused on the development of amino acid-derived ligands for the ATH of ketones. Amino acids are inexpensive starting materials that are readily available from the chiral pool, and the great variety of functionalities gives good possibilities to search for active and selective catalysts. By coupling of a Boc-protected amino acid with an amino alcohol, a pseudo-dipeptide ligand is obtained in a simple one step process (Scheme 5).[42]

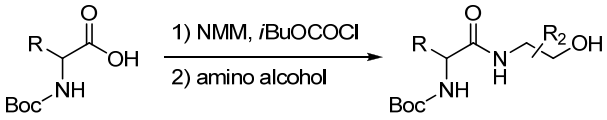

Scheme 5 One-step procedure for the formation of the pseudo-dipeptide ligand.

Combining this type of ligand with a rhodium(III)- or a ruthenium(II)-arene half sandwich complex, generates highly active and selective catalysts for the asymmetric transfer hydrogenation of aromatic ketones. There is a large variety of available amino acids and amino alcohols, which makes the modularity of the ligand immense. A library of differently combined ligands was created.[43] It was shown that the stereochemistry of the amino acid moiety in the ligand strongly influenced the stereochemical outcome of the reduction reaction.[42] The best performing ligands from the library were further studied, and Figure 6 shows the best performing ligands for the rhodium- (**9**) and ruthenium- (**10**) catalyzed ATH, respectively.

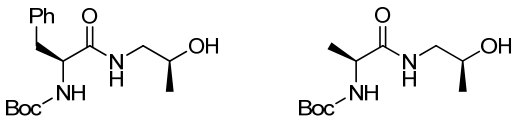

9 **10**

Figure 6 Best performing ligands for the rhodium and ruthenium-catalyzed transfer hydrogenation of ketones.

A structure activity relationship study was performed for the pseudo-dipeptide ligands in the ATH reaction. The ligands were varied in terms of substitution pattern and acidity, and it was demonstrated that all of the functional groups present in the ligands are of high importance for the catalytic activity (Figure 7). Protection of the N-terminus by any group except a carbamate led to loss of activity, alkylation of the internal amide gave a completely inactive catalyst, and any variations in the *C*-terminal OH resulted in catalysts showing little or no activity.[43]

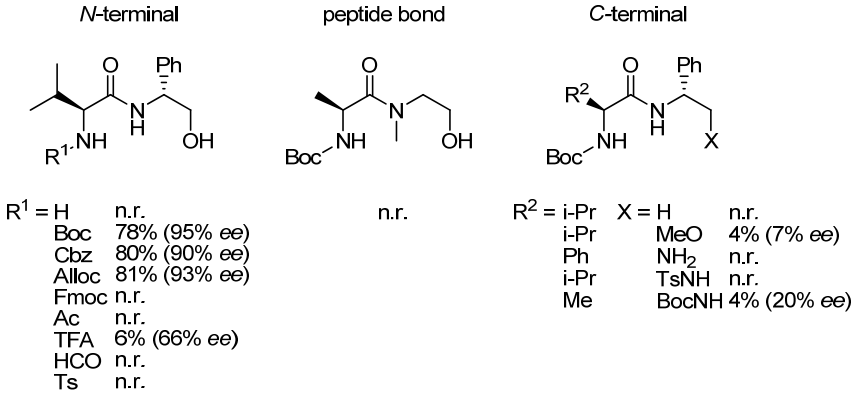

Figure 7 Structural variation of pseudo-dipeptide ligands and catalytic activity in the ruthenium-catalyzed ATH of acetophenone.

It is known that the addition of achiral promoters to a catalytic system can improve the reaction characteristics dramatically.[44] In the pseudo-dipeptide protocol the introduction of an alkali ion along with the base had a direct effect on the outcome of the reaction, and studies were performed on the effects of the nature of additional metal ions to the reaction mixture. The addition of strong Lewis acids, such as scandium triflate or titanium isopropoxide, or addition of copper or silver salts had a negative influence on the reaction, while addition of the alkali salts potassium chloride and sodium chloride gave similar results as the reaction performed without additives. Notably, reactions performed in the presence of added lithium chloride resulted in increased enantioselectivity. The effect is explained by a six-membered transition state analogous to the MPV reaction, in which the smaller lithium ion allows a tighter transition state, inducing a more compact and more sterically defined environment, which has a positive effect on the enantioselectivity of the reaction (Figure 8).[45]

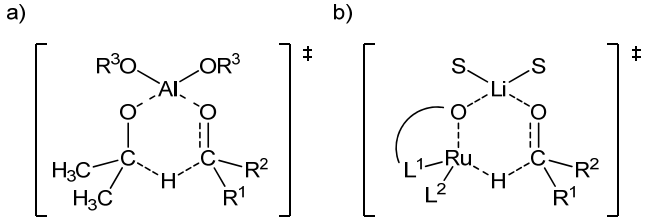

Figure 8 Proposed transition state for the a) MPV reaction and b) ATH with the Ru pseudo-dipeptide catalyst.

All attempts to isolate these ruthenium pseudo-dipeptide complexes for X-ray crystallographic characterization have been unsuccessful, and to gain further knowledge of the ruthenium pseudo-dipeptide-catalyzed ATH reaction, a more detailed mechanistic investigation was performed.

2.1 Results and discussion

2.1.1 Kinetic investigations

The reduction of acetophenone in 2-propanol catalyzed by the combination of [Ru(*p*-cymene)Cl_2]$_2$ and ligand **10** was chosen as a model system for the kinetic analysis. Initially the concentration effects of acetophenone and 2-propanol were examined, and the formation of 1-phenylethanol over time was plotted for a series of different acetophenone concentrations under otherwise identical reaction conditions. From these data the initial rates for the individual runs were plotted as a function of the acetophenone concentration (Figure 9). The plot clearly shows that the reaction rate is dependent on the concentration of acetophenone.

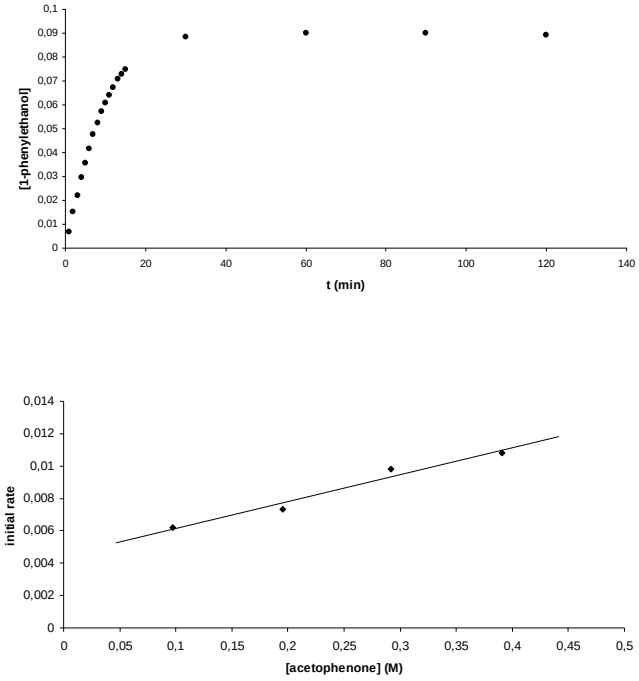

Figure 9 a) Representative plot of a typical reaction profile for the ATH of acetophenone. b) Initial rate *vs.* initial acetophenone concentrations.

Next, the influence of different H donor concentrations on the initial rate was examined. In order to keep the concentration of the acetophenone constant while varying the concentration of 2-propanol, a co-solvent was required. THF was chosen as the additional solvent, since it had earlier been shown that it could be added to the reaction mixture without any negative effects.[46] It was expected that the reaction rate would be directly proportional to the concentration of the donor, but when plotting the initial rates against the corresponding 2-propanol concentrations, we saw that addition of THF actually increased the initial rate (Figure 10). This effect is highest at a 1:1 ratio of 2-propanol and THF. The positive effects of THF addition could be explained by a better solvation of the catalyst, which would give a higher active catalyst concentration, while the hydride donor, 2-propanol, is still in large excess.

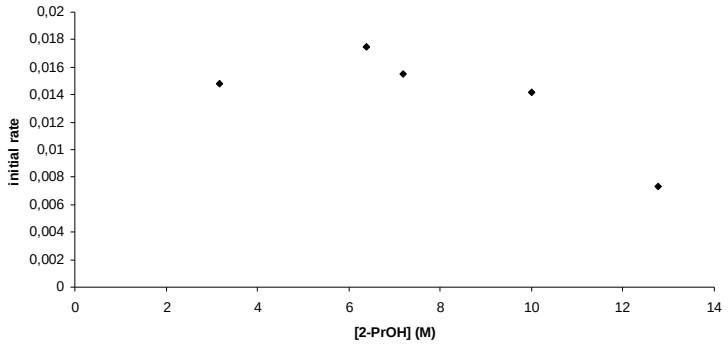

Figure 10 Initial rate *vs.* 2-propanol concentration in the ATH of acetophenone.

A series of experiments was carried out to study the influence of the LiCl concentration on the initial rates of the ATH reactions. Plotting the initial rates versus the LiCl concentration revealed that even a small amount of LiCl gives a dramatic rate acceleration of the reduction reaction (Figure 11). The effect diminishes at higher concentrations and seems to be saturated at 0.2 M.

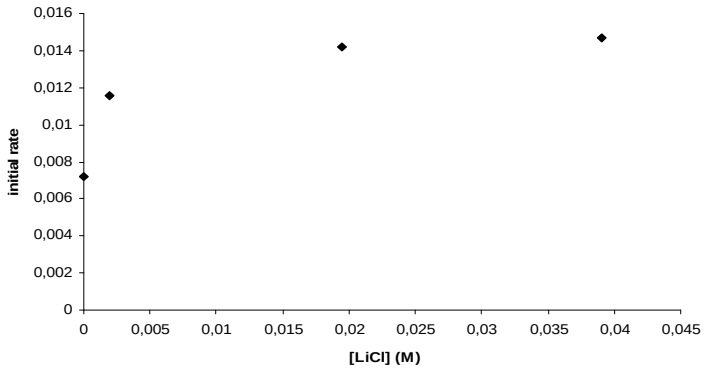

Figure 11 Initial rate *vs.* lithium chloride concentration in the ATH of acetophenone.

2.1.2 Overall kinetic analysis

To obtain a deeper understanding of the mechanism, the data from the initial rate studies were used to determine the rate constants for the individual steps of the reaction. The overall reaction could be divided into two steps (Scheme 6): 1) the reaction between the ruthenium catalyst and 2-propanol to form the active ruthenium hydride and 2) the reaction of Ru-H and acetophenone to form the product and to regenerate the Ru-catalyst.

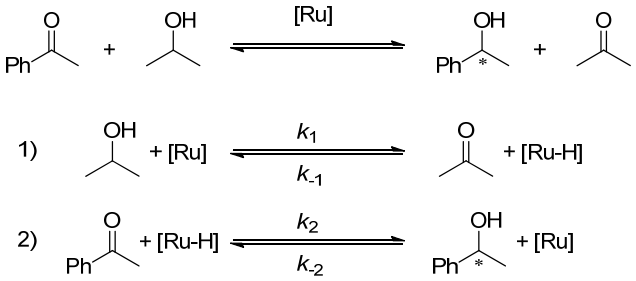

Scheme 6 Schematic representation of the overall process and the two individual steps.

A pseudo-steady-state assumption for the catalyst concentration gave equation 1.

$$[Ru]_{tot} = [Ru] + [Ru\text{-}H] \qquad \text{Eq 1}$$

The overall rate expression can be represented as in equation 2.

$$\frac{\text{rate}}{[Ru]_{tot}} = \frac{k_1 k_2 [2\text{-}PrOH][AcPh] - k_{-1}k_{-2}[Acetone][1\text{-}PhEtOH]}{k_1[2\text{-}PrOH] + k_2[AcPh] + k_{-1}[Acetone] + k_{-2}[1\text{-}PhEtOH]} \qquad \text{Eq 2}$$

At an early stage of the reaction, the concentration of acetone and 1-phenylethanol is zero and the expression can be simplified to equation 3. Equation 3 predicts that the observed order in acetophenone and 2-propanol depends on their relative concentrations. At very low concentrations of acetophenone, k_2[AcPh] << k_1[2-PrOH] and the reaction can be simplified to rate/$[Ru]_{Tot}$ = k_2[AcPh] where the transfer of the hydride from the metal to the substrate becomes the rate determining step. On the other hand, when the concentration of acetophenone is high and k_2[AcPh] >> k_1[2-PrOH] the equation is simplified to rate/$[Ru]_{Tot}$ = k_1[2-PrOH] and formation of the metal hydride becomes rate determining. In the concentration range of these experiments both the terms are of similar size, and both steps are partially rate-limiting throughout the reaction.

$$\frac{\text{rate}}{[Ru]_{tot}} = \frac{k_1 k_2 [2\text{-}PrOH][AcPh]}{k_1[2\text{-}PrOH] + k_2[AcPh]} \qquad \text{Eq 3}$$

Inversion of equation 3 gives equation 4, and by plotting $[Ru]_{Tot}$/rate against 1/[acetophenone] a linear relationship is obtained. The rate constants k_1 and k_2 can be determined from the plot, in which the slope is $1/k_2$ and the intercept is $1/k_1$[2-PrOH].

$$\frac{[\mathrm{Ru}]_{tot}}{\text{rate}} = \frac{1}{k_1[2\text{-PrOH}]} + \frac{1}{k_2[\mathrm{AcPh}]} \qquad \text{Eq 4}$$

The rate constants for the two reverse steps can also be determined. Since the transfer hydrogenation in 2-propanol is an equilibrium reaction, the full rate expression needs to be considered. Once k_1 and k_2 are known, k_{-1} can be determined by measuring the initial rates at different acetone concentrations at a constant acetophenone concentration. Equation 2 can be simplified to equation 5. Inversion of equation 5 and plotting $[\mathrm{Ru}]_{Tot}$/rate *versus* the concentration of acetone gives k_{-1}.

$$\frac{\text{rate}}{[\mathrm{Ru}]_{tot}} = \frac{k_1 k_2 [2\text{-PrOH}][\mathrm{AcPh}]}{k_1[2\text{-PrOH}] + k_2[\mathrm{AcPh}] + k_{-1}[\mathrm{Acetone}]} \qquad \text{Eq 5}$$

When k_1, k_2 and k_{-1} are known, k_{-2} can be determined using the equilibrium equation 6.

$$K_{eq} = \frac{k_1 k_2}{k_{-1} k_{-2}} = \frac{[\mathrm{Acetone}][1\text{-PhEtOH}]}{[2\text{-PrOH}][\mathrm{AcPh}]} \qquad \text{Eq 6}$$

Since the reactions were run to equilibrium, the full reaction profile was available. The experimental data were modeled using DynaFit, a kinetic modeling software.[47] Eight different runs containing 152 data points were simultaneously fitted to provide the values of the individual rate constants in Equation 2. The rate constants obtained are presented in Table 1, and are compared to the measured values. Both the initial rate data and the simulated profiles are in agreement with each other and fit the proposed model (Scheme 6).

Table 1 Kinetic rate constants for the Ru-catalyzed ATH of acetophenone.

	k_1 ($M^{-1}min^{-1}$)	k_2 ($M^{-1}min^{-1}$)	k_{-1} ($M^{-1}min^{-1}$)	k_{-2} ($M^{-1}min^{-1}$)
Initial rate data	1.02	129	85.5	4.70
Modeled data	1.4 ± 0.06	252 ± 17	125 ± 10	5.34 ± 0.26

2.1.3 Kinetic isotope effects

ATH experiments with different hydrogen sources, $(CH_3)_2CHOH$, $(CD_3)_2CDOD$ and $(CH_3)_2CDOH$, were performed, in which the reactions were initiated with sodium *tert*-butoxide instead of isopropoxide to avoid H/D scrambling. The reactions were monitored over time by GLC analysis,

and the initial rates were determined. From the initial rates the following kinetic isotope effects could be measured: k_{CHOH}/k_{CDOH}=4.54, k_{CHOH}/k_{CDOD}=4.42 and k_{CDOD}/k_{CDOH}=1.03. The values indicate a significant KIE for the hydrogen transfer, and the magnitudes of the KIEs are in the same range as for similar ATH systems.[48] The KIE for the system with the fully deuterated donor is of the same order of magnitude as that with $(CH_3)_2CDOH$. Of the two processes involved in transfer hydrogenation reactions, the hydride and the proton transfer, these KIEs clearly show that the rate-limiting step is the hydride transfer, and the small difference when the two deuterated donors are compared indicates that a classical outer sphere mechanism is not operating.

2.1.4 Different ruthenium precursors

It is known that the arene fragment of the ruthenium source can affect the activity and the selectivity of the resulting catalyst.[49] We decided to compare the standard precursor, [Ru(*p*-cymene)Cl_2]$_2$, with two sterically different Ru-arene complexes, [Ru(benzene)Cl_2]$_2$ and [Ru(HMB)Cl_2]$_2$ (HMB = hexamethyl benzene). Both the *p*-cymene and the benzene-containing complexes resulted in active catalysts, while the reaction catalyzed by the more hindered complex with the HMB arene was very slow (Figure 12). The turnover frequency (TOF) with [Ru(*p*-cymene)Cl_2]$_2$ is higher than with[Ru(benzene)Cl_2]$_2$, 153 h^{-1} compared to 70.5 h^{-1} at 30 minutes. Examining the enantioselectivity for the different ruthenium precursors showed that the less hindered [Ru(*p*-cymene)Cl_2]$_2$ and [Ru(benzene)Cl_2]$_2$ gave the secondary alcohol with 96% *ee* and 95% *ee*, respectively, while the [Ru(HMB)Cl_2]$_2$ gave the product with a moderate selectivity of 85%.

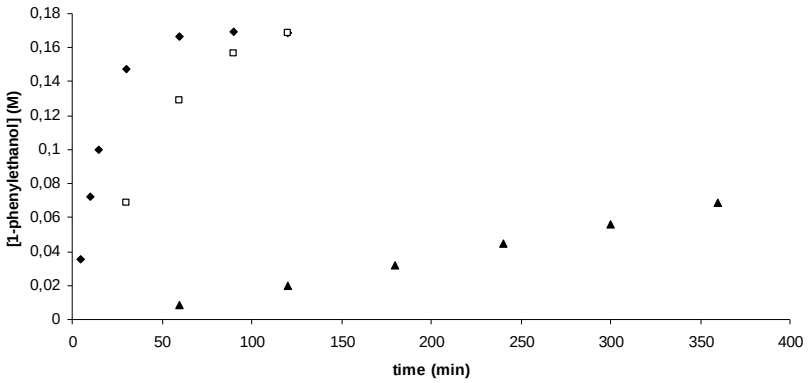

Figure 12 Comparison of different Ru-arene sources in the ATH of acetophenone. (■ [Ru(*p*-cymene)Cl_2]$_2$, □ [Ru(benzene)Cl_2]$_2$ and ▲ [Ru(HMB)Cl_2]$_2$).

2.1.5 Mechanistic models

The pseudo-dipeptide ligands differ from ligands normally employed together with ruthenium arene complexes in that they are potentially tridentate, while other successful ligands are generally bidentate. The pseudo-dipeptide has three functional groups that can act as donors to the metal, and according to the structure activity study they seem to do so. Two of the sites are deprotonated by the alkoxide base and coordinate to the metal in an anionic fashion, while the carbamate functionality binds in a neutral fashion (Figure 13).

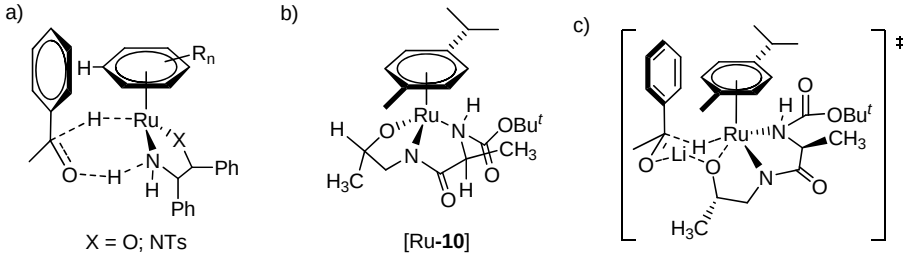

Figure 13 a) Proposed transition state for the reduction of aromatic ketones with a Ru-arene complex of monotosylated diamines or amino alcohols. b) Proposed structure of Ru(*p*-cymene) complex with ligand 8. c) Proposed transition state for the simultaneous transfer of hydride and lithium ion.

Since three equivalents of base are needed to obtain an efficient reaction and only two equivalents are needed in the formation of the complex, it was concluded that the third equivalent is required in a different process.[43b] A significant acceleration in rate is observed upon addition of lithium chloride to the system, whereas removal of alkali metal ions with crown ethers or cryptands reduces the activity. The alkali ion thus needs to be closely bound in the hydrogen transfer process. We have proposed that the transfer of the hydride between 2-propanol and the ruthenium catalyst occurs in a similar fashion as in the MPV reaction (Figure 8). The release of the ligand alkoxide allows for a transfer of the alkali ion to the oxygen of the ligand, and at the same time for coordination of the hydride from the hydrogen donor to the ruthenium center. This mechanism is in line with the observed KIE that can only be associated with the transfer of the hydride, and not the proton transfer. The KIE could also indicate an inner sphere mechanism, but such a process would require two empty coordination sites on the metal, and is therefore unlikely. It would also be highly unlikely that addition of the alkali ions would have a large influence on the selectivity and activity of the reaction if it proceeds via an inner sphere mechanism.

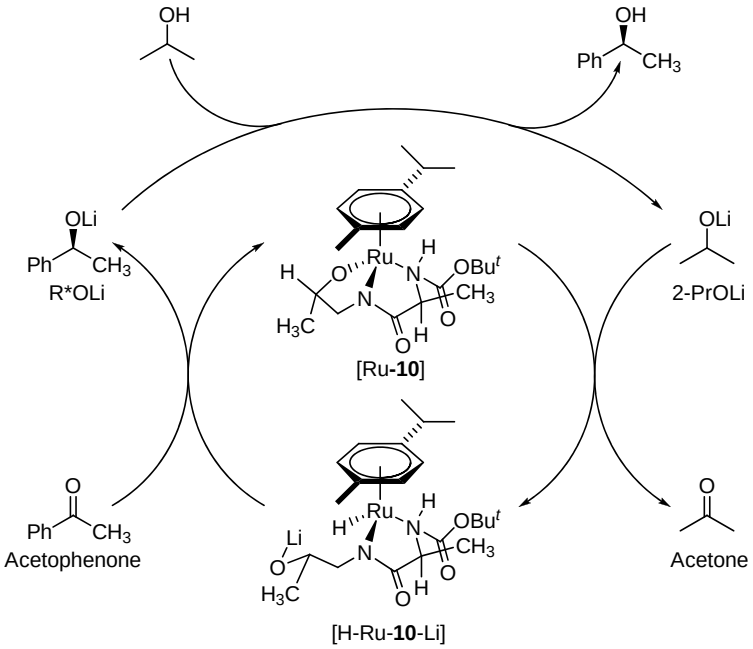

Scheme 7 Proposed catalytic cycle for the [Ru-**10**]-catalyzed ATH in 2-propanol.

Based on the results from our previous studies, as well as the kinetic studies presented above, a new bimetallic mechanism for the ATH reaction catalyzed by the bifunctional [Ru-**10**] catalyst in 2-propanol (Scheme 7) was proposed. The hydrogen donor enters the catalytic cycle as an alkali metal alkoxide, and both the hydride and the alkali metal are delivered to the catalyst simultaneously, forming acetone in the process. The substrate then coordinates to the Lewis acidic alkali metal, and the metal hydride attacks the activated ketone. The hydride transfer is believed to occur via a six-membered transition state involving the alkali metal, the substrate and the catalyst (Figure 13, c). The reduced substrate leaves the catalyst, which reenters the catalytic cycle. The increased selectivity in the presence of the lithium ion is attributed to a tighter transition state formed with the smaller cation.

2.1.6 Substrate scope

As a result of the finding that the ATH process was more efficient using a mixture of 2-propanol and THF, the scope of the reaction was studied at a lower catalyst loading than in previous experiments. Several substituted acetophenones were evaluated with a low catalyst loading of 0.5 mol%. Both electron rich and electron poor substrates were reduced with yields up to 89% and with excellent *ee* in all cases (Table 2).

Table 2 Substrate scope for the Ru pseudo-dipeptide-catalyzed ATH.

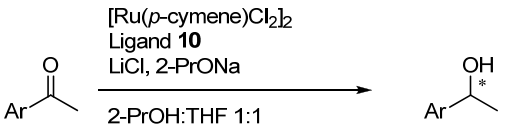

Entry	Substrate	t (min)	Yield (%)[b]	*ee* (%)[c]
1	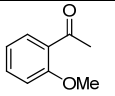	60	45	>99 (S)
2	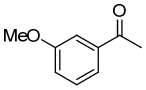	30	80	>99 (S)
3	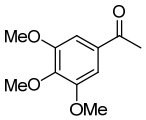	45	79	98 (S)
4		30	70	>99 (S)
5		45	75[d]	>99 (S)
6	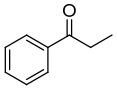	90	82	98 (S)
7	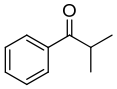	120	18[d]	>99 (S)
8	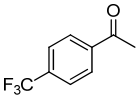	15	89	96 (S)

[a] Reaction conditions: $[Ru(p\text{-cymene})Cl_2]_2$ (0.25 mol%), ligand **10** (0.55 mol%), LiCl (10 mol%), substrate (1 mmol) 2-PrONa (5 mol%) in 2-PrOH:THF 1:1, (5 mL) at 30 °C [b] Isolated yields. [c] Enantioselectivity was determined by GLC analysis (CP Chirasil DEX CB). [d] Conversion determined by GLC analysis.

2.2 Conclusions

We have proposed a new bimetallic outer-sphere mechanism for the ruthenium pseudo-dipeptide-catalyzed ATH of aromatic ketones, in which a hydride and a lithium ion are transferred simultaneously between the catalyst and the substrate/hydrogen donor, in a six-membered transition state. The overall kinetics of the reaction were determined, and the rate constants for the individual steps of the reaction were established. KIE experiments show that the rate determining step of the reaction only involves the transfer of the hydride. The experimental and the modeled data from the kinetic study are in agreement with the proposed mechanism. We were also able to use the information from the study to optimize the reaction conditions further. With addition of lithium chloride to the reaction mixture, and by running the reaction in a solvent mixture of THF and 2-propanol, the catalyst loading could be halved (to 0.5 mol%)compared to our previous reports, and a variety of aromatic ketones could be reduced with excellent enantioselectivity.

3. Selective reduction of heteroaromatic ketones: A combinatorial approach (Paper II)

Our group has reported several amino acid based ligand classes for the ATH of aromatic ketones, which have been employed with 2-propanol, ethanol and formate salts as hydrogen donors. These ligand classes involve functionalities like pseudo-dipeptides, thioamides, hydroxamic acids, sulfinamides and amido triazoles, and they all give good to excellent yields and selectivities.[12b, 42-43, 50]

Normally a catalytic system is developed for one benchmark substrate – essentially different ligands and metals are compared for the reaction of this substrate. In the ATH reaction the most commonly used benchmark substrate is acetophenone, and the optimization of the system is then followed by a substrate screening. These catalysts usually show some generality, and work well for structurally similar substrates, while when the compound of interest is not very similar to the benchmark substrate, poorer results are generally obtained. Using this methodology, there is a high probability that for structurally different substrates, another catalyst could outperform the one found to be optimum for the ATH of the benchmark substrate.

Enantiomerically pure secondary alcohols containing heteroaromatic substituents are commonly employed structural elements in the preparation of biologically active compounds. Such targets are accessible via the asymmetric reduction of the corresponding ketones, and therefore the development of highly selective catalytic protocols for their formation is desirable. Heteroaromatic ketones are generally more challenging substrates in this reaction, due to the possibility for the heteroatom to coordinate to, and thereby inhibit the catalytic activity of, the metal center.

With the large amount of structurally different ligands available to us, we decided to make a two-dimensional screen in which a library of different ligands, and five different heteroaromatic ketones were chosen. Considering the large amount of experiments, a high throughput screening using automated techniques was found to be beneficial.

3.1 Results and discussion

3.1.1 Reaction parameters

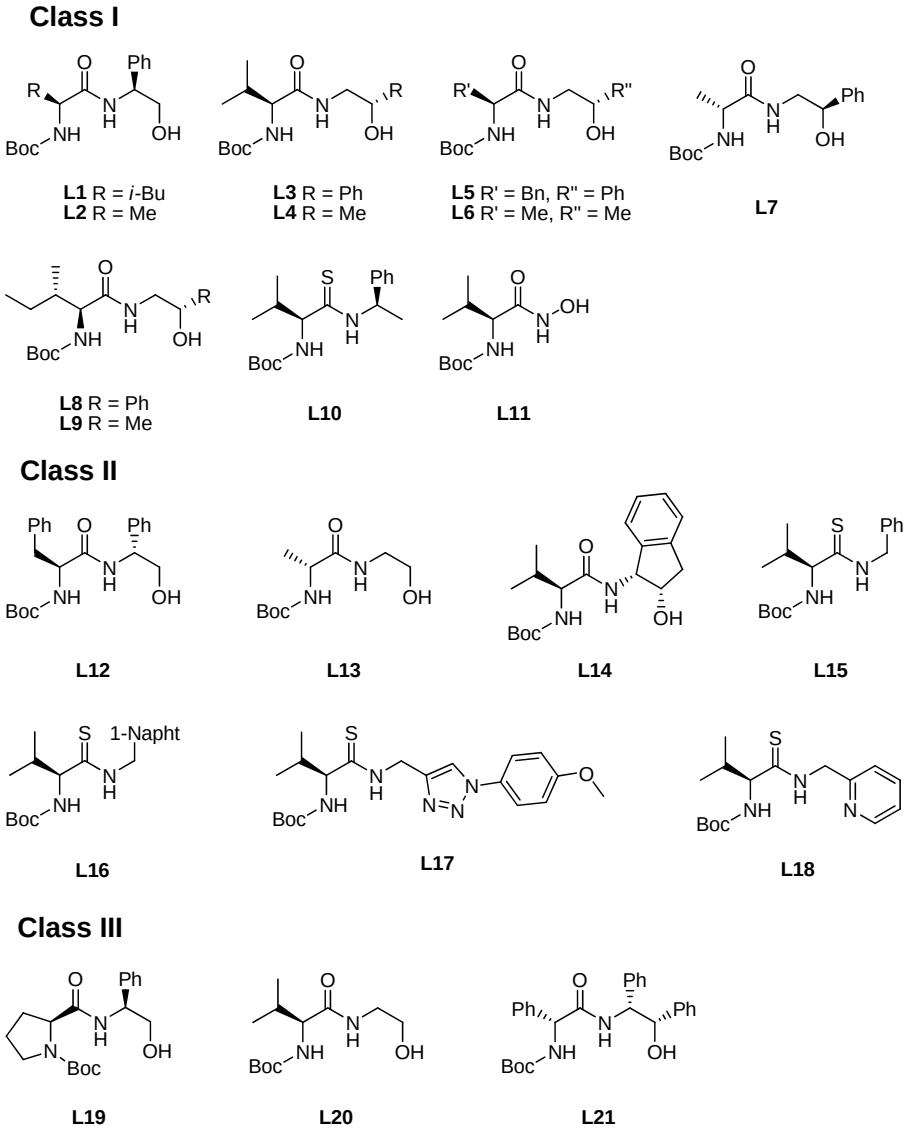

Figure 14 Ligands chosen for the multiple screening for the ATH of heteroatomic ketones.

From our library of around 200 previsouly evaluated ligands, 154 were chosen, and 3D structures were generated using energy minimization.[51] Thereafter, numerous physiochemical 2D and 3D descriptors were calculated for

each ligand, and the descriptor data was subjected to a principal component analysis (PCA).[52, 53] 21 ligands were selected of the score plot generated, to give as much physiochemical diversity as possible. The ligands were classified into three different classes, depending on previous results obtained from the reduction of acetophenone (Figure 14). *Class I*, represent ligands in which the catalyst gave rise to conversion and *ee* >90% (**L1** – **L11**), *class II*, consist of ligands where conversion and *ee* were >60% (**L12** – **L18**), and *class III*, represent ligands where the conversion was <60% and the *ee* >60% (**L19** – **L21**).

The heteroaromatic ketones 2-acetylfuran, 2-acetylthiophene, 3-acetylpyridine, 2-acetylpyridine and 2-acetylpyrazine were chosen as representative models for individual classes of commonly used heterocyclic compounds. These ketones were subjected to the general conditions for the ATH of acetophenone depicted in Scheme 8, – 21 chosen ligands where combined with the half sandwich complexes $[Ru(p\text{-cymene})Cl_2]_2$ and $[Rh(Cp^*)Cl_2]_2$, and the activities and the selectivities of the formed catalysts were evaluated in the reduction reaction. All catalytic reactions were performed on a Chemspeed automated platform under nitrogen atmosphere during a reaction time of 2 h.

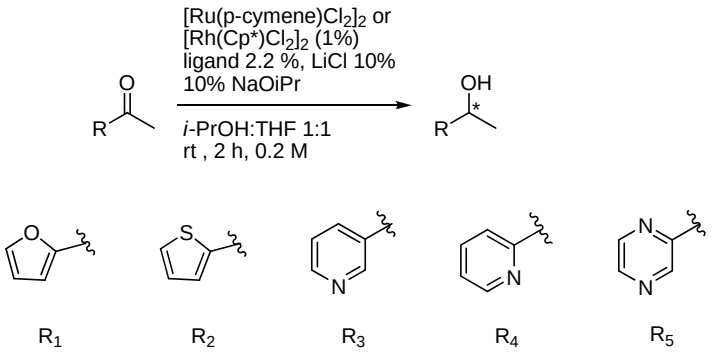

Scheme 8 Conditions for the asymmetric transfer hydrogenation of the heteroaromatic ketones in the screening study.

3.1.2 Evaluation of the multidimensional screening

As can be seen in Figure 15, the reduction of 2-acetylfuran resulted in good to excellent conversions with most of the evaluated catalysts, however, the enantioselectivity is generally poor to moderate throughout the entire series. The combination of the hydroxamic acid ligand **L11** with the ruthenium precursor gave the overall best result with 92% conversion and 88% *ee*.

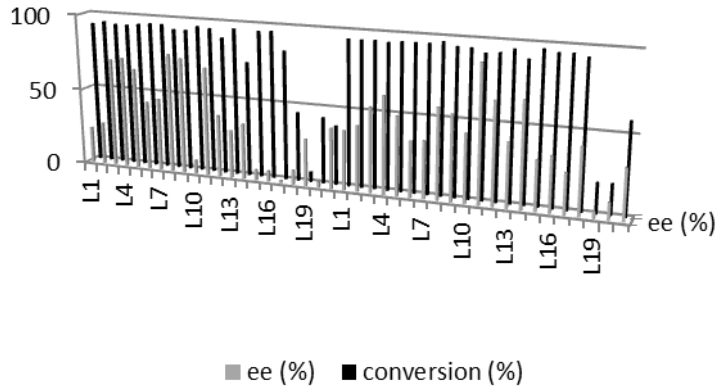

Figure 15 Screening results for 2-acetylfuran with the rhodium-catalyzed reactions on the left, and ruthenium-catalyzed reactions on the right.

Similar results were observed in the reduction of 2-acetylthiophene (Figure 16), in which most of the class I/II catalysts gave conversions above 70%, with enantioselectivities ranging between 45 and 88%, and the catalysts derived from class III ligands led to less satisfactory results. The best result was obtained using the combination of **L8** and $[Rh(Cp^*)Cl_2]_2$ (80% conversion and 86% *ee*).

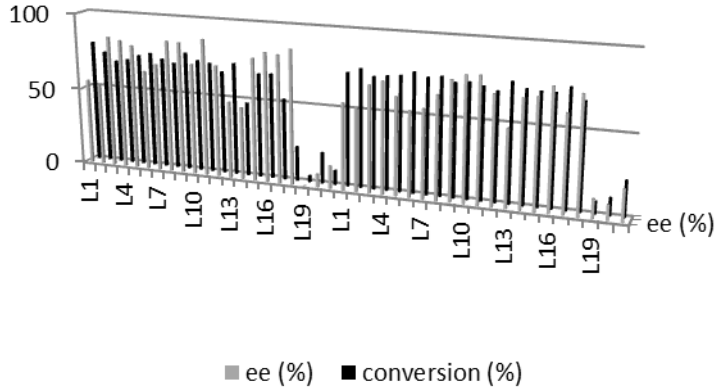

Figure 16 Screening results for 2-acetylthiophene with the rhodium-catalyzed reactions on the left, and ruthenium-catalyzed reactions on the right.

The majority of the class I/II catalysts gave conversions higher than 90%, with enantioselectivities above 85% in the reduction of 3-acetylpyridine (Figure 17). Generally, the rhodium catalysts performed better than the ruthenium analogues, and the catalysts generated from class III ligands were

inferior when compared to catalysts derived from class I in particular. The overall best result was obtained using the rhodium catalyst formed with **L3**, which gave a conversion of 98% and 97% *ee*.

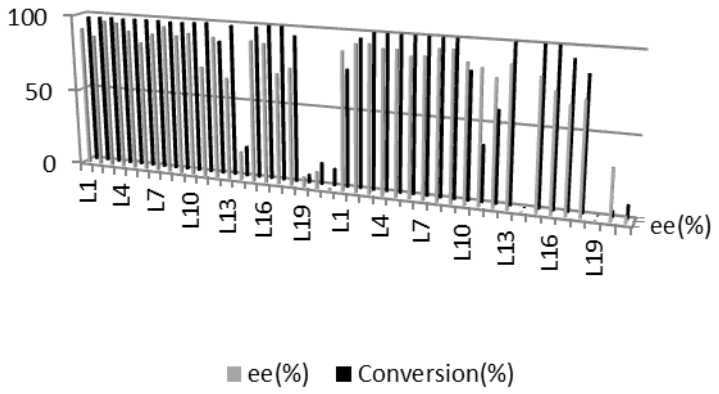

Figure 17 Screening results for 3-acetylpyridine with the rhodium-catalyzed reactions on the left, and ruthenium-catalyzed reactions on the right.

The heterocyclic substrate 2-acetylpyrazine (Figure 18), proved to be most difficult to reduce using the amino acid based rhodium or ruthenium catalysts. Among the class I/II catalysts, it was only the rhodium complexes of thioamide ligands along with the hydroxamic acid ligand **L11** that showed any activity. The Rh-complex of the thioamide ligand **L17** demonstrated the highest catalytic activity for this ketone with 36% conversion and 99% *ee*.

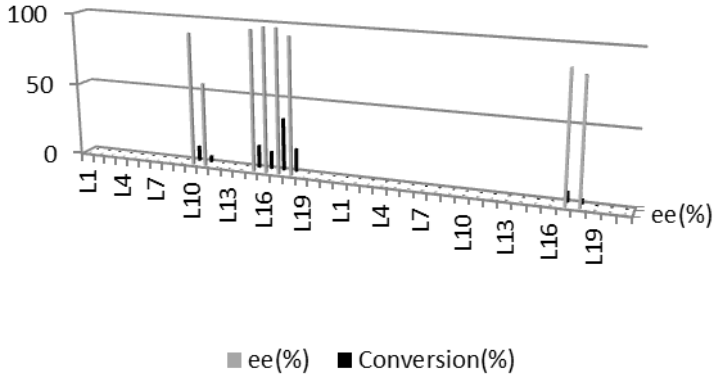

Figure 18 Screening results for 2-acetylpyrazine with the rhodium-catalyzed reactions on the left, and ruthenium-catalyzed reactions on the right.

For 2-acetylpyridine, only the conversions are available, and not the enantioselectivities due to HPLC instrument problems, but the activities of the catalysts formed are quite demonstrative (Figure 19). Most of the formed catalysts give quite low conversions, with the exception of the thioamides. All thioamide containing ligands in the study gave almost full conversion to the corresponding alcohol, while the traditionally well performing pseudo-dipeptides gave lower conversions.

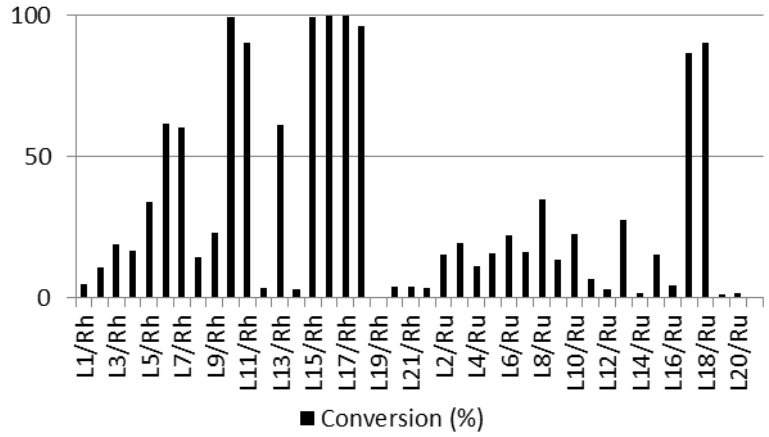

Figure 19 Screening results for 2-acetylpyridine with the rhodium-catalyzed reactions on the left, and ruthenium-catalyzed reactions on the right.

The limited number of catalysts that were active in the transfer hydrogenation reaction for coordinating substrates is not surprising. Previous attempts to obtain crystal structures for the pseudo-dipeptide ligand complexes have failed, suggesting that the ligands do not bind strongly to the metal center. Since the two nitrogens in the pyrazine substrate can coordinate to the metal catalyst, it can be assumed that they readily compete with the ligands. The exception is the hydroxamic acid ligand and the thioamide ligands which are assumed to bind more tightly to the metal center, especially to rhodium. This finding is also in line with previous work in which a crystal structure was successfully obtained for thioamide **10** with rhodium.[50d] The considerably lower enantioselectivities compared to the simple substrate acetophenone can probably be ascribed to coordination of the heteroatom to the metal center, leading to a decrease in catalyst selectivity. This effect is most pronounced when the heteroatom is placed next to the ketone, as could be expected.

These results clearly show that the optimum catalyst for the transfer hydrogenation of acetophenone is not necessarily the most suitable one for structurally and electronically different ketones. There is a risk that catalysts or conditions for more complex substrates can be discarded, due to inferior results for the structurally simpler substrate. A multidimensional screening, like the one performed here, is an excellent way to circumvent this problem. After finding the optimal catalyst for each substrate class, the information could subsequently be used to select the most appropriate catalysts for the synthesis of more complex structures containing that basic motif.

3.1.3 Formal syntheses of biologically active compounds

With the knowledge obtained from the screening process described above, we decided to perform the asymmetric key step in a formal synthesis of the two antidepressant drugs fluoxetine and duloxetine (Figure 20), which contain an acetophenone and a 2-acetylthiophene core, respectively.

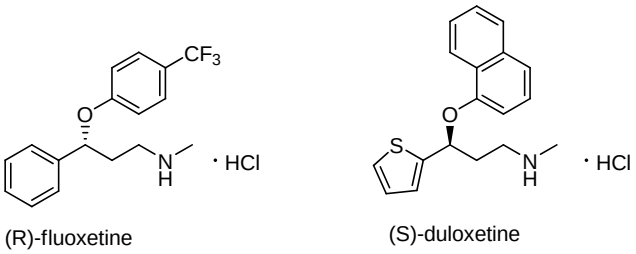

Figure 20 Antidepressants (*R*)-fluoxetine (Prozac) and (*S*)-duloxetine (Cymbalta).

In accordance with literature procedures, Mannich reactions were performed reacting the ketones **11 a-b** with formaldehyde and methylamine hydrochloride under acidic conditions.[54] The Mannich products **12 a-b** were then protected with Boc-anhydride resulting in 47 % and 42 % yield of **13a** and **13b**, respectively, over two steps (Scheme 9).

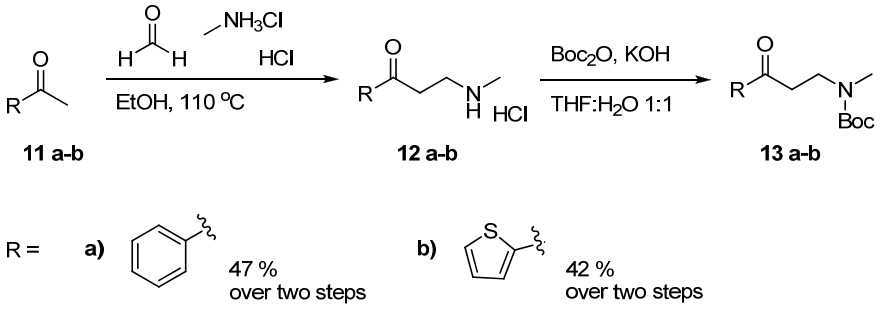

Scheme 9 Mannich reaction followed by Boc protection.

For the ATH of the two ketones we selected the most appropriate catalysts based on the results we obtained for the structurally similar substrates during the preceding catalyst screening (Scheme 10). (*R*)-Fluoxetine is an acetophenone analogue, and the best performing catalyst for acetophenone was chosen, a combination of ligand 6 (Figure 14) together with the ruthenium precursor. To achieve the desired enantiomer, the ligand derived from the non-natural amino acid and the *R*-amino alcohol was chosen. With a catalyst loading of 5 mol%, and a concentration of 0.05 M to drive the equilibrium towards complete formation of the alcohol, the reaction gave the desired alcohol **14 a** in a high 94% yield and with excellent enantioselectivity of >99% after 60 minutes. For the synthesis of (*S*)-duloxetine, we selected the catalyst that had proven most successful in the ATH of structurally similar acetyl thiophene for use in the reduction step, combining rhodium and the pseudo-dipeptide ligand 8 (Figure 14). The concentration of the reaction was lowered to 0.01 M compared to 0.2 M employed in the screening process, and after 90 minutes, the corresponding alcohol **14 b** was isolated in a 94% yield with >99% enantioselectivity.

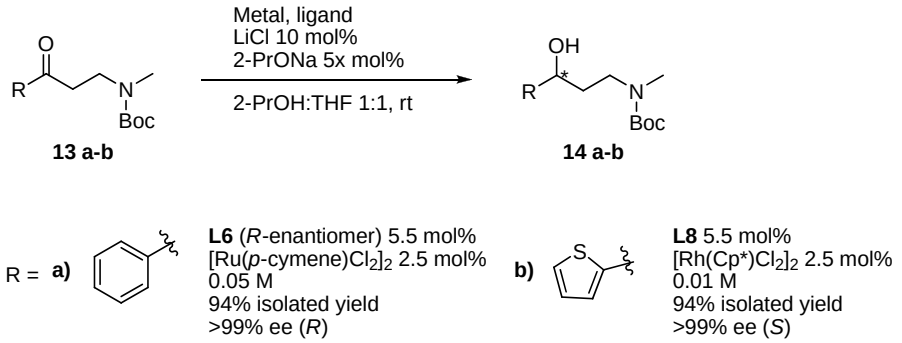

Scheme 10 ATH with the optimized catalysts for the syntheses of (*R*)-fluoxetine and (*S*)-duloxetine.

Subsequent ring closure to the cyclic carbamates **15 a-b**,[55] hydroxide deprotection to **16 a-b**[56] followed by classic S_NAr arylation of the aminoalcohol[57] and HCl crystallization in accordance with literature procedures would lead to the target molecules (Scheme 11).

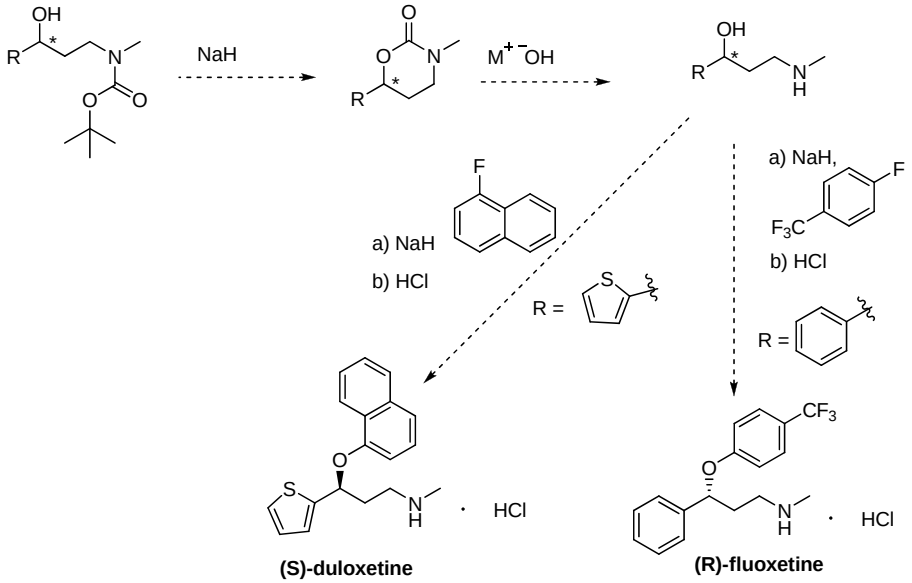

Scheme 11 Formal synthesis of enantioenriched (*R*)-fluoxetine and (*S*)-duloxetine from the Boc protected alcohols.

3.3 Conclusions

A high throughput, multidimensional screening of catalysts from a library of highly modular amino acid-based ligands was performed, and optimal catalysts were identified for five different classes of heteroaromatic ketones, illustrating that a catalyst which gives the best results for a model substrate is not always the best catalyst in general. The knowledge obtained from the multidimensional screen was used in the key step of the formal syntheses of (R)-fluoxetine and (S)-duloxetine, where the key reduction steps resulted in isolated yields of 94 %, and >99% *ee* for both compounds.

4. A simple and selective iron-NHC-catalyzed hydrosilylation of ketones (Paper III)

Most catalysts today are derived from heavy or rare metals and the toxicity and high price of those are major drawbacks for large scale synthesis. Recently, it has been shown that copper complexes and iron complexes can be used as benign alternatives to the traditionally used complexes. Iron being the most naturally abundant metal, is both inexpensive as well as environmentally and biologically compatible.[58] Until recently, iron has been relatively underrepresented in the field of catalysis compared to other transition metals, but lately there has been an increase of its use, and there are nowadays several efficient processes reported that can compete with other transition metal-catalyzed procedures.[59]

Iron-catalyzed reductions of ketones are traditionally performed under harsh conditions,[59] but today there are several mild hydrosilylation protocols available for this transformation. The first examples of iron-catalyzed hydrosilylation were reported by Brunner in the early 90's, who used half sandwich iron complexes for the transformation.[60] Nishiyama and Furuta later showed that the combination of $Fe(OAc)_2$ with TMEDA or thiophene ligands gave active catalysts for the reduction of ketones, and they also reported the first enantioselective iron-catalyzed hydrosilylation of ketones, although with moderate *ee*s.[61]

Beller and co-workers have developed efficient phosphine-based systems for the reduction of aldehydes and ketones using $Fe(OAc)_2$ together with PCy_3, and later showed that using (*S*,*S*)-Me-Duphos instead of PCy_3 gave enantiomerically enriched products in the reduction of aryl ketones.[62] Gade described the synthesis of well-defined iron complexes containing tridentate, enantiopure ligands for the use in hydrosilylation under similar conditions as those reported by Nishiyama and Furuta.[63] Chirik reported the use of highly active, well defined iron complexes for the efficient and selective hydrosilylation of ketones with very low catalyst loadings.[64] In 2010, Tilley showed that a simple iron complex with hexamethyldisilazane as a ligand, generated a highly active catalyst for the reduction of aldehydes and ketones.[65]

Ligands based on *N*-heterocyclic carbenes (NHCs) are frequently used as alternatives to phosphines in a number of catalytic applications. NHCs are strong σ-donors, but weak π-acceptors, which makes them particularly useful in catalytic processes where electron rich metal complexes are required.[66] NHCs serve as spectator ligands that influence the catalysis by steric and electronic effects, but they do not directly bind the substrates.

Imidazol-2-ylidenes were the first family of stable NHCs to be isolated, the first one by Arduengo in 1991 (Figure 21).[67] They are usually prepared by deprotonation of the corresponding imidazolium salt with a strong base; the pK_a of the conjugate acid is approximately 24 in DMSO.[68] NHCs are known to coordinate to alkali metals, main group elements, transition metals and lanthanides. The use of NHC ligands in combination with iron for carbonyl reductions would result in the formation of intermediate iron hydrides in which the iron hydrogen bond has strong ionic character, hence it would be highly hydridic.

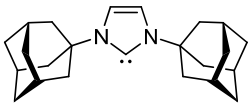

Figure 21 The first isolated stable carbene, the Arduengo carbene.

In 2010, Royo's group reported the tethered half sandwich complex **17** (Figure 22), which performed well in the catalytic hydrosilylation of electron poor aldehydes.[69]

Taking a similar approach, the group of Darcel and Sortais initiated an investigation derived from the piano stool iron complex prepared by Guerchais in 2003 (Figure 22).[70] They presented a catalytic system which could reduce aldehydes, ketones, and even imines in high yields.[71]

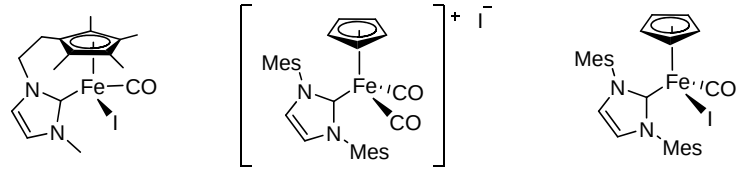

17 **18** **19**

Figure 22 Royo's and Sortais/Darcel's half sandwich iron complexes.

4.1 Results and discussion

Our intention was to generate an Fe-NHC catalyst for hydrosilylation reactions *in situ* by combining an iron salt with an *N*-heterocyclic carbene (NHC) as a ligand additive. The NHCs were generated by treatment of a series of azolium and azolidinium salts with base. The salts chosen for the study are all commercially available or easily synthesized from readily available starting materials (Figure 23). The optimization work was conducted on acetophenone as the model substrate using different silanes, different iron sources and modifying various reaction parameters, such as the temperature, the stoichiometry as well as the metal and ligand precursors.

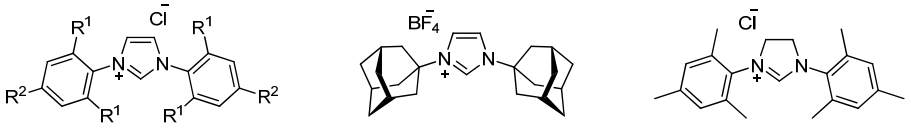

Figure 23 NHC precursors used in the optimization studies for the iron-catalyzed hydrosilylation.

4.1.1 Optimization of the catalytic system

Initially, a 1 mol% loading of $Fe(OAc)_2$ was combined with IMes·HCl and sodium *tert*-butoxide in a ratio of 1:2:2 in THF, with acetophenone as the model substrate, and 4 equivalents of the polymeric silane PMHS (Table 3). These conditions resulted in 61% conversion of the substrate into 1-phenylethanol after basic work-up. Similar results were obtained with $(EtO)_2MeSiH$, while the use of diphenylsilane gave significantly lower conversion. Increasing the catalyst loading led to higher conversions, and interestingly, the screening of bases showed that the use of potassium *tert*-butoxide gave an even higher conversion. After establishing the initial parameters we focused on the NHC ligands. IMes·HCl, IPr·HCl, IAd·BF_4 and SIMes·HCl all gave active catalysts when combined with iron acetate, but the best result was obtained with IPr·HCl. As previously observed by Beller,[62a] the use of other iron salts resulted in catalysts with very poor activity. We then turned our attention towards the solvent, temperature and iron:ligand ratio, and we saw that using non-ether solvents or running the reaction at low temperatures resulted in very low conversions. The iron:NHC ratio could be reduced to 1:1.2 without loss of any activity, but when adding less than 3 equivalents of silane, the conversion dropped slightly.

Table 3 Optimization for the reduction of acetophenone.[a]

Entry	Fe (mol%)	L (mol%)	Base (mol%)	Silane (equiv)	Conv (%)
1	1	IMes·HCl (2)	*t*BuONa (2)	PMHS (4)	61
2	1	IMes·HCl (2)	*t*BuONa (2)	$(EtO)_2MeSiH$ (4)	63
3	1	IMes·HCl (2)	*t*BuONa (2)	Ph_2SiH_2 (4)	88
4	2.5	IMes·HCl (5)	*t*BuONa (5)	PMHS (4)	78
5	2.5	IMes·HCl (5)	*t*BuOK (5)	PMHS (4)	87
6	2.5	IAd·HBF_4 (5)	*t*BuOK (5)	PMHS (4)	93
7	2.5	SIMes·HCl (5)	*t*BuOK (5)	PMHS (4)	69
8	2.5	IPr·HCl (5)	*t*BuOK (5)	PMHS (4)	94
9	2.5	IPr·HCl (3)	*t*BuOK (3)	PMHS (3)	94
10	-	IPr·HCl (3)	*t*BuOK (3)	PMHS (3)	<5
11	-	-	*t*BuOK (3)	PMHS (3)	99
12	2.5	IPr·HCl (3)	*n*BuLi (3)	PMHS (3)	99
13	-	IPr·HCl (3)	*n*BuLi (3)	PMHS (3)	<5
14	-	-	*n*BuLi (3)	PMHS (3)	<5
15[c]	2.5	IPr·HCl (3)	*n*BuLi (3)	PMHS (3)	99

[a] General conditions: acetophenone (1 mmol), $Fe(OAc)_2$, NHC-precursor, base and silane according to the table, THF (3 mL), 65 °C, 16 – 18 h. Hydrolytic work-up with NaOH (2 M, aq). [b] Conversion determined by GLC analysis. [c] $Fe(OAc)_2$ 99.995% based on trace metal analysis was employed.

Without addition of any NHC precursor the reaction did not proceed, and running the reaction without any iron present gave an exceptionally low conversion. On the other hand, when running the reaction only in the presence of the alkoxide base the product was formed in high yield. Since alkoxide bases are known to catalyze the hydrosilylation reaction of carbonyl compounds,[72] a final optimization was performed where we used *n*-BuLi for the deprotonation of the imidazolium salt. Using *n*-BuLi, the risk for a base-catalyzed background reaction was completely avoided, and we saw that the reaction proceeded with full conversion. After a basic work-up, 1-phenylethanol was isolated in 89% yield.

1.2 Substrate scope

Using the optimized conditions for the hydrosilylation a large variety of ketones, both aromatic and aliphatic, were reduced (Table 4). Both electron rich and electron poor aromatic ketones were reduced in good to excellent yields. Functional groups that are susceptible to reduction, such as C-F bonds and NO_2, remained unreacted under these reaction conditions. Ester groups withstood the conditions but an alternative work-up with TBAF was required to avoid hydrolysis. The catalytic system also worked well for synthetically useful heteroaromatic ketones. Furthermore, aliphatic ketones were also reduced in high yields.

Table 4 Substrate scope for the iron-NHC-catalyzed hydrosilylation of ketones.

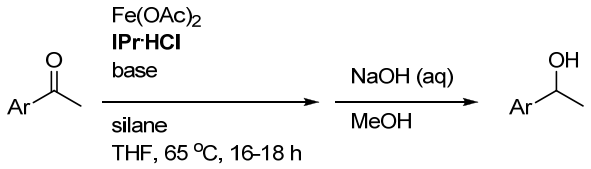

Entry	Substrate	Yield (%)[b]	Entry	Substrate	Yield (%)[b]
1	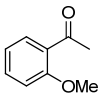	>99[c]	**11**	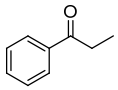	83
2	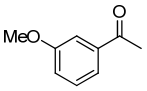	53[c]	**12**	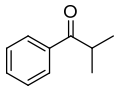	91
3	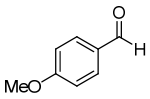	96	**13**	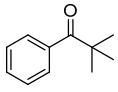	55

4	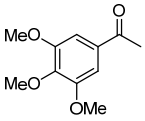	89[c]	**14**		89
5	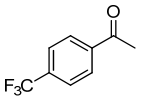	>99[c]	**15**		>99[c]
6	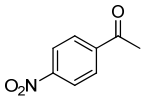	94[c]	**16**		75[c]
7	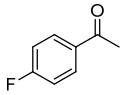	92	**17**	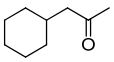	66
8	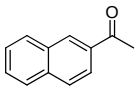	97	**18**	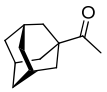	94
9	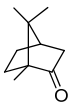	81[d]	**19**	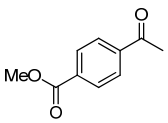	87
10		81	**20**	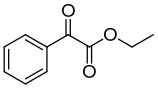	70

[a] General conditions: ketone (1 mmol), *n*-BuLi (3 mol%), $Fe(OAc)_2$ (2.5 mol%), IPr·HCl (3 mol%), THF (3 mL), PMHS (3 equiv.), 65 ºC, 16-18 h. Hydrolysis of the initially formed silyl ether was performed using NaOH in H_2O for 2 h [b] Isolated yields [c] Conversion determined by GLC. [d] Diastereomeric ratio (isoborneol:borneol, 8:1) measured by ^{1}H-NMR.

4.2 Conclusions

An effective and general iron-NHC-catalyzed hydrosilylation protocol has been developed. The catalyst was easily generated *in situ* by treatment of an azolium salt with a base in the presence of an iron source, and all of the reagents are commercially available. The catalyst system was suitable for reducing aromatic ketones, aliphatic ketones and heteroaromatic ketones and the mild protocol showed a high functional group tolerance.

5. Iron-catalyzed hydrosilylation of carbonyl compounds with hydroxyethyl NHC ligands (paper IV)

A frequently encountered limitation of the iron-catalyzed protocols, including the one developed by us, is the low activity of the catalysts. The reaction times are often long, and the reaction temperatures elevated. In an attempt to shorten these reaction times for the iron-NHC system, a set of sterically less demanding NHC precursors was prepared. These ligands were, in addition to being less hindered, also potentially bidentate, with a hydroxyethyl moiety, which could possibly stabilize the catalyst further, and thereby increase the activity.

Three different imidazolium salts were prepared (Figure 24), all of them of considerably reduced size, where two of them had the above mentioned hydroxyl moiety. This set of NHC precursors was then evaluated as ligands for the iron-catalyzed hydrosilylation of ketones.

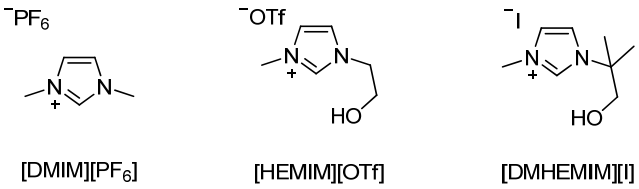

Figure 24 NHC precursors for the iron-catalyzed HS.

5.1 Results and discussion

5.1.1 Synthesis of the ligands

The ligands were easily prepared using short reaction procedures. For the synthesis of [DMIM][PF_6], 1-methyl imidazole was treated with iodomethane, followed by treatment with potassium hexafluorophophate, to perform the ion exchange. The hydroxyethyl imidazolium salts were prepared as

presented in Scheme 12. Alkylation of imidazole **20**, initially with chloroethanol, and subsequently by methyl triflate in a second step, yielded [HEMIM][OTf]. The preparation of the dimethyl analogue, [DMHEMIM], was initiated by formation of 1-(1-ethoxycarbonylethyl)imidazole **22** according to the procedure of Bellemin-Laponnaz and Gade,[73] followed by reduction of the ester with LAH to form the alcohol **23**, and subsequent alkylation with iodomethane.

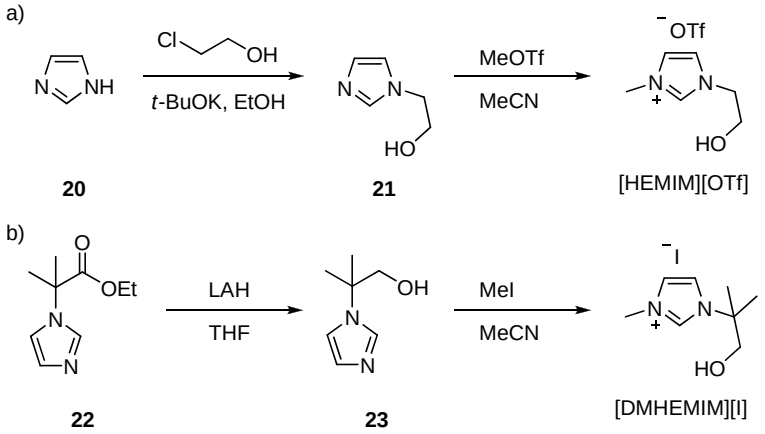

Scheme 12 Synthesis of the ligand precursors [HEMIM][OTf] and [DMHEMIM][I].

5.1.2 Optimization of the catalytic system

Initially, the imidazolium salts were employed in the iron-catalyzed hydrosilylation under the same conditions as the ones optimized for the commercially available IPr·HCl (Table 4). The use of [DMIM][PF_6], gave results comparable to those previously reported, but when introducing the hydroxyethyl substituted salts, dramatically more active catalysts were formed. Using 2.5 mol% of the non-substituted hydroxyethyl imidazolium salt, [HEMIM][OTf], full conversion was reached after only a 15 min reaction time. The catalyst loading could be decreased to 1 mol% without affecting the outcome of the reaction, and full conversion was still reached after only 30 minutes. Employing the dimethyl substituted analogue [DMHEMIM][I], led to a somewhat longer reaction time, although with full conversion still achieved after only 60 min when using 1 mol% catalyst. The incredible increase in activity encouraged us to lower the reaction temperature, and it was observed that even at room temperature the reaction ran to completion, although a prolonged reaction time of 18 hours was needed. To evaluate the influence of the hydroxyl group in the potentially bidentate ligand, the reaction was run using the ligand precursor **24** where the hydroxyl was protected with a tosyl group, and after two hours no conversion could be observed. To

make sure that the reaction was not catalyzed by either the ligand or the metal source alone, we ran the reaction under such conditions individually, and indeed, the starting material remained unreacted. As expected, no reaction occurred with only the silane. The purity of the iron in all the experiments was 99.995%, to make sure that no traces of other metals could be involved in catalyzing the transformations.

Table 5 Hydrosilylation of acetophenone catalyzed by *in situ* generated iron complexes.[a]

Entry	Ligand precursor	Fe (mol%)	Time (h)	Temp (°C)	Conv. (%)[b]
1	[DMIM][PF_6]	2.5	18	65	>99
2	[HEMIM][OTf]	2.5	0.25	65	>99
3	[HEMIM][OTf]	1	0.5	65	>99
4	[HEMIM][OTf]	2.5	18	22	>99
5	[DMHEMIM][I]	1	1	65	>99
6	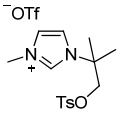 **24**	2.5	2	65	-
7	-	2.5	18	65	-
8	[HEMIM][OTf]	-	2	65	-

[a] General conditions: $Fe(OAc)_2$, ligand precursor, *n*-BuLi, (Fe:L:Base, 1:1.1:2.2) substrate 2 mmol, THF (5 mL) and PMHS (3 equiv.). Hydrolysis of the initially formed silyl ether was performed using NaOH in H_2O for 2 h. [b] Conversion determined by ^{1}H-NMR.

5.1.3 Substrate scope

Using the optimized conditions for the hydrosilylation a variety of aldehydes and ketones, either aromatic, heteroaromatic or aliphatic, were reduced with short reaction times below 180 minutes. The reaction conditions and the results for the screen are presented in Table 6. The aldehydes reacted rapidly to form the corresponding primary alcohols. Both electron-rich and electron-deficient aromatic ketones were reduced in good to excellent yields. Ester groups withstood the conditions but an alternative workup with TBAF was required to avoid hydrolysis. The catalytic system also worked well for synthetically useful heteroaromatic ketones. Furthermore, aliphatic ketones were reduced in high yields.

Table 6 Hydrosilylation of aldehydes and ketones catalyzed by $Fe(OAc)_2$ and [HEMIM]-[OTf].

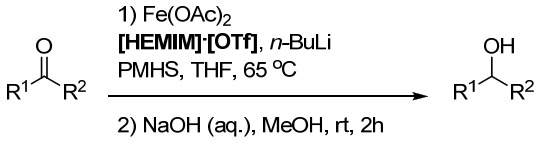

Entry	Substrate	Time (min)	Yield (%)[b]	Entry	Substrate	Time (min)	Yield (%)[b]
1	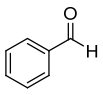	10	>99[c]	**9**		150	78
2	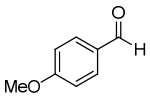	30	>99[c]	**10**	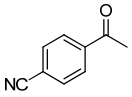	60	93
3	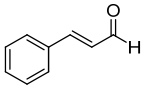	60	>99[c]	**11**		60	91
4	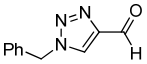	60	>99[c]	**12**		30	79
5	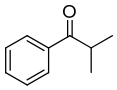	30	81	**13**		60	90
6	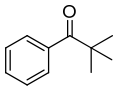	60	85	**14**		60	98
7		120	85	**15**	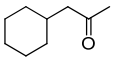	180	85
8[d]	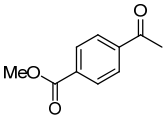	120	85	**16**	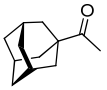	120	92

[a] General conditions: $Fe(OAc)_2$ (1 mol%), [HEMIM][OTf] (1.1 mol%), n-BuLi (2.2 mol%), substrate 2 mmol, THF (5 mL) and PMHS (3 equiv.). Hydrolysis of the initially formed silyl ether was performed using NaOH in H_2O for 1 h. [b] Isolated yields. [c] Conversion determined by ^{1}H-NMR. [d] Hydrolytic work-up using TBAF.

5.2 Conclusions

A general and efficient protocol for the iron-NHC-catalyzed hydrosilylation was presented in which the active catalyst was generated *in situ* by treatment of a hydroxyethyl imidazolium salt with a base in the presence of an iron source. The system proved to be very effective, and low catalyst loadings and short reaction times were observed. The catalyst system was able to reduce aromatic, heteroaromatic and aliphatic aldehydes and ketones in high yields, and furthermore, the mild protocol showed high functional group tolerance.

6. Efficient iron-NHC-catalyzed reduction of tertiary amides to amines (Appendix B)

Amines are exceedingly common functionalities found in essentially all pharmaceuticals (Figure 25), and the most common methods of connective C-N bond formation are by reductive amination (from a carbonyl and an amine) or amidation followed by reduction (from a carboxylic acid and an amine) which typically employ aluminum or boron hydride reagents. The direct reduction of amides to amines without the use of these hydride reagents is a highly attractive transformation,[74] and in recent years, large effort has been put into development of transition metal-catalyzed reductions of amides. Several transition metal-catalyzed hydrolsilylaton protocols for the reduction of amides have been reported, one of the first was described by Ito in 1998, in which he used an analogue of Wilkinson's rhodium catalyst for the reduction of tertiary amides.[75] The operational simplicity of this type of reaction has led to several other examples emerging, which employ a variety of different transition metals.

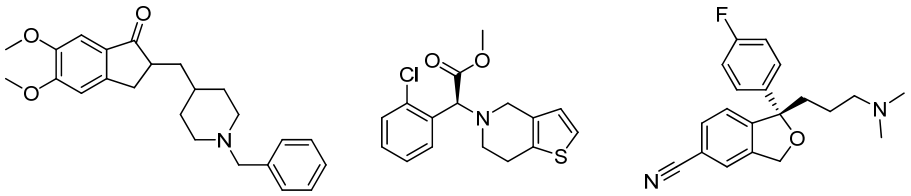

Figure 25 Amine containing top selling pharmaceuticals in the US during 2010.[76]

Recently, Beller has reported on copper-[77] and zinc-[78] based systems for the reduction of secondary and tertiary amides. Iron, being the most abundant transition metal and having a low toxicity, has become an interesting alternative for this transformation, and there are some recent examples.

Beller showed that the iron carbonyl complex [$Fe_3(CO)_{12}$] could be used together with PMHS for the direct reduction of tertiary amides to amines at 100 °C.[79] Simultaneously, the group of Nagashima also reported that the iron carbonyl complexes [$Fe(CO)_5$] and [$Fe_3(CO)_{12}$] could be used for the reduction. The reaction could be carried out under both thermal and photoassisted conditions, using either PMHS or TMDS as the reducing agent. They also

observed that in the presence of a nitro group, the amide functionality remained completely untouched throughout the reaction, and the nitro functionality was selectively reduced.[80] Nagashima's group also showed that when employing BDSB as the hydride source instead, the reaction times could be decreased, and the catalyst loading lowered.[81] The cationic piano stool complexes published by Sortais and Darcel were shown to be active in the reduction of secondary and tertiary amides at elevated temperatures.[71a] Recently, Beller also presented a reduction of primary amides to amines, using a combination of two iron complexes, together with a phenanthroline ligand. Combination of $[Et_3NH][HFe_3(CO)_{12}]$ with iron acetate gave the corresponding amines in a two-step reaction, in which the iron carbonyl complex reduced the amides to nitriles, followed by reduction of the newly formed nitriles to the amines by iron acetate.[82]

Considering the high activity of the iron hydroxyethyl/NHC-based system for the catalytic reduction of amides to amines, we decided to evaluate this catalyst in the hydrosilylation of amides.

6.1 Results and discussion

Initially, we chose *N*,*N*-dimethylbenzamide as the benchmark substrate, and subjected it to the same conditions as the ones we reported for the HS of ketones and aldehydes. For the amide to react, a prolonged reaction time was required. Full conversion of the starting material could be observed after 16 hours, although we could also observe formation as benzyl alcohol. This promising result encouraged us to investigate the conditions further, in an attempt to improve the outcome of the reaction.

Initially the reaction was performed with 2.5 mol% of the iron source, but the catalytic loading could be decreased to 1 mol% without diminishing the activity. There was no difference in activity or selectivity observed when comparing the ionic liquid [HEMIM][OTf] to the phenyl substituted analogue **25** (Figure 26), while the substituted imidazolium salt is a solid, and therefore easier to handle and was thus chosen for further optimizations.

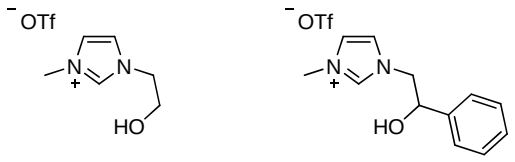

[HEMIM][OTf] **25**

Figure 26 Hydroxyethyl imidazoles used as ligand precursors in the iron-NHC-catalyzed reduction of amides.

A series of different silanes were compared to the originally used PMHS, in an attempt to improve the selectivity of the reaction. This optimization proved to be fruitless, except for when employing triethoxysilane, which gave a clean reaction. However, due to the higher price, and the hazards involved with it,[83] we chose to continue our studies with PMHS as the hydride source, trying to optimize the conditions to avoid the formation of by-products (Table 7).

We believed that the high amount of benzyl alcohol formed in the reaction could be due to water being present in the mixture, and decided to add drying agents to circumvent this problem. Addition of molecular sieves and magnesium sulphate completely inhibited the reaction, while with sodium sulphate present, the reaction progressed with full conversion to product, atlhough together with the byproduct. Neither changing the concentration of the reaction, nor varying the amount of PMHS led to a reaction without formation of benzyl alcohol. When running the hydrosilylation in dioxane, no reaction was observed, while the reaction in toluene led to a full conversion, but with a high amount of benzyl alcohol formed.

Table 7 Optimization of the reaction conditions for the iron-catalyzed reduction of *N*,*N*-benzylamide.[a]

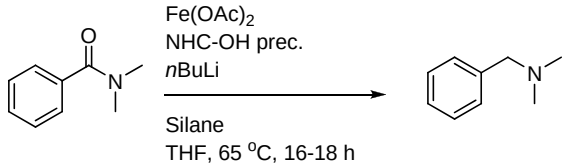

Entry	Fe (mol%)	Ligand	Silane	Solvent	Conv (%)[b]	Sel (%)[c]
1	5	IPr·HCl	PMHS	THF	>99	70
2	2.5	HEMIM	PMHS	THF	>99	71
3	1	HEMIM	PMHS	THF	>99	58
4	1	PhHEMIM	PMHS	THF	>99	77
5	5	PhHEMIM	PMHS	THF	>99	64
6	-	HEMIM	$(EtO)_3SiH$	THF	>99	89
7	1	PhHEMIM	$(MeO)_3SiH$	THF	Traces	-
8	1	PhHEMIM	TMDS	THF	Full	33
9	1	PhHEMIM	$(EtO)_2MeSiH$	THF	>99	71
10	1	PhHEMIM	PMHS	Dioxan	-	-
11	1	PhHEMIM	PMHS	Toluene	>99	62
12	1	PhHEMIM	$(EtO)_3SiH$	Dioxan	Traces	-
13	1	PhHEMIM	$(EtO)_3SiH$	Toluene	Traces	-

[a] General conditions: $Fe(OAc)_2$, ligand, *n*-BuLi, (Fe:Li:Base, 1:1.1:2.2) solvent (3 mL), *N*, *N*-dimethylbenzamide (1 mmol), silane (3 equiv.), 65 ºC for 16 – 18 h. [b] Conversion determined by ^{1}H-NMR. [c] Selectivity: product amine/total amount of products

When attempting to isolate the corresponding *N*,*N*-dimethylbenzylamine, we were not able to isolate yields in agreement with the observed conversions, regardless of the conditions. We suspected that the problem might have been arising from the fact that dimethylbenzylamine, although having a high boiling point (183 °C), could be volatile enough to partially evaporate during the isolation procedure, and attempted a reduction of piperidylbenzamide instead. The amide was fully reduced under the reaction conditions, and we were pleased to see that almost no benzyl alcohol was formed in the reaction (Scheme 13), and the corresponding amine could be isolated in an 82% yield.

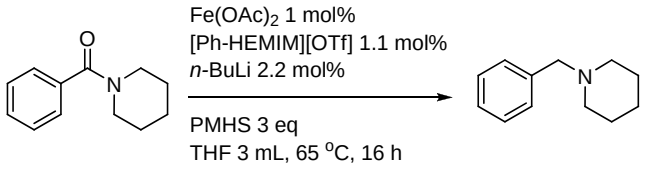

Scheme 13 Optimized conditions for the iron-NHC-catalyzed reduction of amides.

To make sure that the reaction was not catalyzed by either the ligand or the metal source alone, we ran the reaction under such conditions individually, and indeed, the starting material remained unreacted. As expected, no reaction occurred with only the silane. The purity of the iron in all the experiments was 99.995%, to make sure that no traces of other metals could be involved in catalyzing the transformations.

6.2 Conclusions

The previously reported hydroxyethyl-NHC/iron-catalyzed hydrosilylation protocol was proven effective even for the reduction of tertiary aromatic amides. The catalysts were formed *in situ* in a simple manner, and the corresponding amines were obtained in high yields with a low catalyst loading.

Concluding remarks

Isolation of the catalytically active complexes used in the ATH reaction within our group has so far proven elusive, and to gain a better understanding of the system a detailed mechanistic study was performed. Based on kinetic studies, isotope labeling and modeling data, a novel bimetallic outer-sphere mechanism was proposed, in which the hydride and a lithium ion are transferred simultaneously in the rate determining step, in a six-membered transition state. Results from the kinetic study led to further optimization of the catalytic system, since addition of LiCl and THF to the reaction mixture was shown to lead to a large rate enhancement. The positive effects of the additives made it possible to decrease the catalyst loading to 0.5 mol% - half of the amount used previously.

Considering the high abundance of enantiomerically pure secondary alcohols with heteroaromatic substituents, the low number of ATH catalysts known for the reduction of these types of substrates, and the fact that we had access to hundreds of well performing ligands for this transformation, we performed a multi-dimensional screen to find catalysts that work optimally for heteroaromatic ketones. To demonstrate the applicability of the study, we performed formal syntheses of the biologically active compounds (*R*)-fluoxetine and (*S*)-duloxetine, in which the latter contains a heteroaromatic ketone core that was evaluated in our catalyst screening. Choosing the optimal catalysts for these cores from the screen, we were able to reduce both ketones in high yields and with excellent selectivities, indicating the value of such methodology.

Since it is of high interest to replace expensive and toxic transition metals as catalyst, we started to investigate a system for the iron-catalyzed hydrosilylation. Commercially available azolium salts were used for the *in situ* formation of NHCs, and were examined as alternatives for the commonly used phosphine ligands with good results. There are only a limited number of iron-catalyzed hydrosilylation protocols available in which NHC ligands are engaged, and our system is operationally very simple. Both the iron source and the silane are inexpensive and benign, and the system proved to be wide-ranging in terms of tolerated substituents on the ketones, although the reaction times were quite long.

When employing a sterically less demanding NHC ligand with a hydroxyethyl handle, which makes the ligand potentially bidentate instead, we saw a dramatic acceleration of the reaction rate. With low catalyst loading the system showed enhanced catalytic activity compared to other similar systems, and the scope of the tolerated substituents remained very wide. With the high activity of the *in situ* formed catalyst, we believed it could be possible to reduce even more demanding carbonyls, and indeed, the highly active iron-hydroxyethyl NHC system was also proven to be suitable for the reduction of tertiary amides to amines, a transformation where it is highly attractive to avoid the use of reactive hydride reagents. There is still room for improvement in the amide reduction protocol, and ideally the system could be extended to both secondary and primary amides.

Acknowledgements

There are people I would like to thank:

Professor Hans Adolfsson, för din vägledning och ditt förtroende under de här åren, för att jag fått chansen att utvecklas som självständig tänkare och för att du tagit dig tid att förklara det som har varit svårt. Tack för ditt ständigt goda humör och alla erfarenheter jag fått under den här tiden!

Professor Jan-Erling Bäckvall för det intresse du visat för mitt arbete.

Dr Jenny Wettergren, Herr Dr Lorenzo Zani, Helena Lundberg, Dr Hans-Göran Andersson, Alexey Volkov, Fredrik Tinnis and *Dr Per Ryberg* for fruitful collaborations.

Paul McGonigal and *Katrin Ahlford* for proofreading and language improvements, you guys make me look good.

Mia och *Anuja*, tack för hjälpen med framsidan!

HA-group, all past and present members. I particularly want to thank *Wettis, Jesper, Lolo* and *Katti* for the warm welcome to the group when I knew nothing about anything, *Helena, Tunnis* and *Alexey*, you have made my last time completely unforgettable. Thank you for all the great memories!

Jag vill tacka för ekonomiskt stöd från Svenska kemistsamfundet, KSLA, Ångpanneföreningens forskningsstiftelse, K & A Wallenbergs minnesfond, Astra Zeneca, stiftelserna till minne av Hilda Rietz, L & E Kinander och John Söderberg.

TA-personalen, för all er hjälp med att laga saker, använda maskiner, diverse blanketter, greja med datorer och så mycket mer, och för att ni alltid har en stund över för småprat.

All my friends and colleagues at the *Department of Organic Chemistry.*
Speciellt er på *kontoret*, dagen blir liksom lite bättre i gott sällskap!

Professor Antonio Echavarren, for the opportunity to spend time in your lab and work on a great project. I also want to thank all the people in the *Echi lab*, and at the rest of the *ICIQ*, for an amazing atmosphere. I especially want to thank *Mädz* for kindly saving my life, *Johansson* - you are wise as an abuelo, and *Riccardo* for your unwavering support and enthusiasm, you are truly diabolic!

Jag vill tacka mina vänner.
Ni finns på många platser i världen och i min närhet. Jag träffar ingen av er så ofta som jag skulle vilja, men ni finns i mina tankar, och ni gör motgångar hanterbara och ni gör både vardag och fest oförglömligt.

Nazli, från första dagen har du stått vid min sida i stora och små ögonblick. Utan dig hade det inte varit roligt att göra den här grejen. Tack för allt under de här nio åren, du är en bra vän!

Jag vill tacka min familj.
Pappa för att du alltid tror på mig och för den hjälp jag har fått när jag har behövt den, och även när jag inte gjort det.
Hanna, du är en väldigt speciell person som är mycket på alla tänkbara sätt. Tack för den inverkan du har haft på mitt liv, jag kan inte tänka mig hur det hade varit utan dig.

Appendix A

The author's contributions to papers I-IV and Appendix B

I. Took part in the optimization of the catalytic system. Performed the substrate evaluation and was involved in the preparation of the manuscript.

II. Took part in planning the experiments for the two-dimensional screening and performed most of the synthetic work. Was involved in the preparation of the manuscript.

III. Performed most of the synthetic work and was involved in the preparation of the manuscript.

IV. Initiated the project, performed most of the synthetic work and was involved in the preparation of the manuscript.

Appendix B Initiated the project and performed most of the synthetic work.

Appendix B

General procedure for the hydrosilylation of amides: $Fe(OAc)_2$ (x mol%) and the NHC precursor (1.1x mol%) were treated with vacuum in a dried tube for 15 min. Dry THF (2 mL) was added to the sealed tube under nitrogen atmosphere, followed by *n*BuLi (2.2x mol%). The substrate amide (1 mmol) in dry THF (1 mL) was added to the mixture, the temperature was increased to 65 °C, and the silane (3 eq.) was added. After 16-18 hours the mixture was cooled to ambient temperature, and NaOH (aq, 2 M, 5 mL) was added. The mixture was stirred for 3 hours, followed by extraction of the product with DCM (3 x 15 mL). The organic phase was dried with Na_2SO_4, the solvent was evaporated and the crude product was analyzed by ^{1}H-NMR.

***N*-benzyl piperidine** was purified by filtration through a neutral alumina column and eluted with ethyl acetate. Yield: 143 mg, 82 % **^{1}H-NMR** (400 MHz, $CDCl_3$): 1.41-1.48 (m, 2H), 1.63-.168 (m, 4H), 2.48 (bs, 4H), 3.59 (s, 2H), 7.24-7.37 (m, 5H) **^{13}C-NMR** (100 MHz, $CDCl_3$): 24.5, 26.1, 54.5, 63.9, 126.8, 128.1, 129.2, 138.7

References

(1) M. A. Hollinger, *Introduction to Pharmacology, Second Edition*, **2003**.

(2) M. Breuer, K. Ditrich, T. Habicher, B. Hauer, M. Kesseler, R. Stuermer, T. Zelinski, *Angew. Chem., Int. Ed.* **2004**, *43*, 788-824.

(3) a) B. Martín-Matute, J.-E. Bäckvall, *Curr. Opin. Chem. Biol.* **2007**, *11*, 226-232; b) B. Martín-Matute, J.-E. Bäckvall, Wiley-VCH Verlag GmbH & Co. KGaA, **2008**, pp. 89-113.

(4) a) P. I. Dalko, L. Moisan, *Angew. Chem., Int. Ed.* **2001**, *40*, 3726-3748; b) I. Dalko Peter, L. Moisan, *Angew. Chem., Int. Ed.* **2004**, *43*, 5138-5175.

(5) a) T. Ohkuma, M. Kitamura, R. Noyori, *Catal. Asymmetric Synth. (2nd Ed.)* **2000**, 1-110; b) T. Ohkuma, M. Koizumi, M. Yoshida, R. Noyori, *Org. Lett.* **2000**, *2*, 1749-1751; c) H.-U. Blaser, C. Malan, B. Pugin, F. Spindler, H. Steiner, M. Studer, *Adv. Synth. Catal.* **2003**, *345*, 103-151.

(6) a) M. J. Palmer, M. Wills, *Tetrahedron: Asymmetry* **1999**, *10*, 2045-2061; b) G. Zassinovich, G. Mestroni, S. Gladiali, *Chem. Rev.* **1992**, *92*, 1051-1069; c) S. Gladiali, E. Alberico, *Chem. Soc. Rev.* **2006**, *35*, 226-236.

(7) a) H. Meerwein, R. Schmidt, *Justus Liebigs Ann. Chem.* **1925**, *444*, 221-238; b) A. Verley, *Bull. Soc. Chim. Fr.* **1925**, *37*, 537-542; c) W. Ponndorf, *Angew. Chem.* **1926**, *39*, 138-143.

(8) R. V. Oppenauer, *Recl. Trav. Chim. Pays-Bas Belg.* **1937**, *56*, 137-144.

(9) M. J. Trocha-Grimshaw, H. B. Henbest, *Chem. Commun.* **1967**, 544.

(10) a) Y. Sasson, J. Blum, *Tetrahedron Lett.* **1971**, 2167-2170; b) Y. Sasson, J. Blum, *J. Org. Chem.* **1975**, *40*, 1887-1896.

(11) R. L. Chowdhury, J. E. Bäckvall, *J. Chem. Soc., Chem. Commun.* **1991**, 1063-1064.

(12) a) N. A. Cortez, G. Aguirre, M. Parra-Hake, R. Somanathan, *Tetrahedron Lett.* **2007**, *48*, 4335-4338; b) K. Ahlford, J. Lind, L. Mäler, H. Adolfsson, *Green Chem.* **2008**, *10*, 832-835; c) C. Bubert, J. Blacker, S. M. Brown, J. Crosby, S. Fitzjohn, J. P. Muxworthy, T. Thorpe, J. M. J. Williams, *Tetrahedron Lett.* **2001**, *42*, 4037-4039; d) T. Thorpe, J. Blacker, S. M. Brown, C. Bubert, J. Crosby, S. Fitzjohn, J. P. Muxworthy, J. M. J. Williams, *Tetrahedron Lett.* **2001**, *42*, 4041-4043; e) X. Li, J. Blacker, I. Houson, X. Wu, J. Xiao, *Synlett* **2006**, 1155-1160.

(13) J. S. M. Samec, J.-E. Bäckvall, P. G. Andersson, P. Brandt, *Chem. Soc. Rev.* **2006**, *35*, 237-248.

(14) O. Pamies, J.-E. Bäckvall, *Chem. Eur. J.* **2001**, *7*, 5052-5058.

(15) a) S. Hashiguchi, A. Fujii, J. Takehara, T. Ikariya, R. Noyori, *J. Am. Chem. Soc.* **1995**, *117*, 7562-7563; b) K.-J. Haack, S. Hashiguchi, A. Fujii, T. Ikariya, R. Noyori, *Angew. Chem., Int. Ed.* **1997**, *36*, 285-288.

(16) a) J. Takehara, S. Hashiguchi, A. Fujii, S.-i. Inoue, T. Ikariya, R. Noyori, *Chem. Commun.* **1996**, 233-234; b) S. J. M. Nordin, P. Roth, T. Tarnai, D. A. Alonso, P. Brandt, P. G. Andersson, *Chem. Eur. J.* **2001**, *7*, 1431-1436.
(17) M. T. Reetz, X. Li, *J. Am. Chem. Soc.* **2006**, *128*, 1044-1045.
(18) a) D. A. Alonso, P. Brandt, S. J. M. Nordin, P. G. Andersson, *J. Am. Chem. Soc.* **1999**, *121*, 9580-9588; b) M. Yamakawa, I. Yamada, R. Noyori, *Angew. Chem., Int. Ed.* **2001**, *40*, 2818-2821.
(19) W. Baratta, G. Chelucci, S. Gladiali, K. Siega, M. Toniutti, M. Zanette, E. Zangrando, P. Rigo, *Angew. Chem., Int. Ed.* **2005**, *44*, 6214-6219.
(20) W. Baratta, M. Bosco, G. Chelucci, Z. A. Del, K. Siega, M. Toniutti, E. Zangrando, P. Rigo, *Organometallics* **2006**, *25*, 4611-4620.
(21) W. Baratta, M. Ballico, G. Chelucci, K. Siega, P. Rigo, *Angew. Chem., Int. Ed.* **2008**, *47*, 4362-4365.
(22) a) P. E. Sues, A. J. Lough, R. H. Morris, *Organometallics* **2011**, *30*, 4418-4431; b) C. Sui-Seng, F. Freutel, A. J. Lough, R. H. Morris, *Angew. Chem., Int. Ed.* **2008**, *47*, 940-943; c) N. Meyer, A. J. Lough, R. H. Morris, *Chem. Eur. J.* **2009**, *15*, 5605-5610; d) A. Mikhailine, A. J. Lough, R. H. Morris, *J. Am. Chem. Soc.* **2009**, *131*, 1394-1395; e) P. O. Lagaditis, A. J. Lough, R. H. Morris, *J. Am. Chem. Soc.* **2011**, *133*, 9662-9665; f) J. F. Sonnenberg, N. Coombs, P. A. Dube, R. H. Morris, *J. Am. Chem. Soc.* **2012**, *134*, 5893-5899.
(23) S. Rendler, M. Oestreich, *Mod. Reduct. Methods* **2008**, 183-207.
(24) J. M. Lavis, R. E. Maleczka, Jr., *e-EROS Encycl. Reagents Org. Synth.* **2001**.
(25) R. J. P. Corriu, J. J. E. Moreau, *J. Chem. Soc., Chem. Commun.* **1973**, 38-39.
(26) a) W. Dumont, J. C. Poulin, P. Dang Tuan, H. B. Kagan, *J. Am. Chem. Soc.* **1973**, *95*, 8295-8299; b) N. Langlois, P. Dang Tuan, H. B. Kagan, *Tetrahedron Lett.* **1973**, 4865-4868.
(27) O. Riant, N. Mostefai, J. Courmarcel, *Synthesis* **2004**, 2943-2958.
(28) J.-F. Carpentier, V. Bette, *Curr. Org. Chem.* **2002**, *6*, 913-936.
(29) a) H. Nishiyama, M. Kondo, T. Nakamura, K. Itoh, *Organometallics* **1991**, *10*, 500-508; b) H. Nishiyama, S. Yamaguchi, M. Kondo, K. Itoh, *J. Org. Chem.* **1992**, *57*, 4306-4309.
(30) T. Langer, J. Janssen, G. Helmchen, *Tetrahedron: Asymmetry* **1996**, *7*, 1599-1602.
(31) L. M. Newman, J. M. J. Williams, R. McCague, G. A. Potter, *Tetrahedron: Asymmetry* **1996**, *7*, 1597-1598.
(32) B. Tao, G. C. Fu, *Angew. Chem., Int. Ed.* **2002**, *41*, 3892-3894.
(33) M. B. Carter, B. Schiott, A. Gutierrez, S. L. Buchwald, *J. Am. Chem. Soc.* **1994**, *116*, 11667-11670.
(34) R. L. Halterman, T. M. Ramsey, Z. Chen, *J. Org. Chem.* **1994**, *59*, 2642-2644.
(35) S. Xin, J. F. Harrod, *Can. J. Chem.* **1995**, *73*, 999-1002.
(36) H. Imma, M. Mori, T. Nakai, *Synlett* **1996**, 1229-1230.
(37) M. Bandini, F. Bernardi, A. Bottoni, P. G. Cozzi, G. P. Miscione, A. Umani-Ronchi, *Eur. J. Org. Chem.* **2003**, 2972-2984.

(38) H. Mimoun, *J. Org. Chem.* **1999**, *64*, 2582-2589.
(39) a) S. Rendler, M. Oestreich, *Angew. Chem., Int. Ed.* **2007**, *46*, 498-504; b) C. Deutsch, N. Krause, B. H. Lipshutz, *Chem. Rev.* **2008**, *108*, 2916-2927; c) O. Riant, Pt. 2 ed., John Wiley & Sons Ltd., **2009**, pp. 731-773; d) M. Zaidlewicz, M. M. Pakulski, *Vol. 2*, Georg Thieme Verlag, **2011**, pp. 59-131.
(40) I. Ojima, M. Nihonyanagi, Y. Nagai, *Bull. Chem. Soc. Jap.* **1972**, *45*, 3722.
(41) I. Ojima, T. Kogure, M. Kumagai, S. Horiuchi, T. Sato, *J. Organomet. Chem.* **1976**, *122*, 83-97.
(42) I. M. Pastor, P. Västilä, H. Adolfsson, *Chem. Commun.* **2002**, 2046-2047.
(43) a) I. M. Pastor, P. Västilä, H. Adolfsson, *Chem. Eur. J.* **2003**, *9*, 4031-4045; b) A. Bøgevig, I. M. Pastor, H. Adolfsson, *Chem. Eur. J.* **2004**, *10*, 294-302.
(44) E. M. Vogl, H. Gröger, M. Shibasaki, *Angew. Chem., Int. Ed.* **1999**, *38*, 1570-1577.
(45) P. Västilä, A. B. Zaitsev, J. Wettergren, T. Privalov, H. Adolfsson, *Chem. Eur. J.* **2006**, *12*, 3218-3225.
(46) J. Wettergren, A. B. Zaitsev, H. Adolfsson, *Adv. Synth. Catal.* **2007**, *349*, 2556-2562.
(47) P. Kuzmic, *Anal. Biochem.* **1996**, *237*, 260-273.
(48) a) C. P. Casey, S. W. Singer, D. R. Powell, R. K. Hayashi, M. Kavana, *J. Am. Chem. Soc.* **2001**, *123*, 1090-1100; b) C. P. Casey, J. B. Johnson, *J. Org. Chem.* **2003**, *68*, 1998-2001.
(49) M. Yamakawa, I. Yamada, R. Noyori, *Angew. Chem., Int. Ed.* **2001**, *40*, 2818-2821.
(50) a) A. B. Zaitsev, H. Adolfsson, *Org. Lett.* **2006**, *8*, 5129-5132; b) K. Ahlford, A. B. Zaitsev, J. Ekström, H. Adolfsson, *Synlett* **2007**, 2541-2544; c) L. Zani, L. Eriksson, H. Adolfsson, *Eur. J. Org. Chem.* **2008**, 4655-4664; d) K. Ahlford, M. Livendahl, H. Adolfsson, *Tetrahedron Lett.* **2009**, *50*, 6321-6324; e) F. Tinnis, H. Adolfsson, *Org. Biomol. Chem.* **2010**, *8*, 4536-4539; f) K. Ahlford, H. Adolfsson, *Catal. Commun.* **2011**, *12*, 1118-1121; g) H. Lundberg, H. Adolfsson, *Tetrahedron Lett.* **2011**, *52*, 2754-2758.
(51) MOE (The Molecular Operating Environment), 2010.10; Chemical Computing Group Inc., 1010 Sherbrooke Street West, Suite 910, Montreal, Canada H3A 2R7, 2010.
(52) S. Wold, K. Esbensen, P. Geladi, *Chemom. Intel. Lab. Sys.* **1987**, *2*, 37-52.
(53) Evince, 2.3.0; Umbio AB: Box 7980, 90719 Umeå, Sweden, 2009
(54) D. Liu, W. Gao, C. Wang, X. Zhang, *Angew. Chem., Int. Ed.* **2005**, *44*, 1687-1689.
(55) a) R. Millet, A. M. Träff, M. L. Petrus, J.-E. Bäckvall, *J. Am. Chem. Soc.* **2010**, *132*, 15182-15184; b) S. G. Davies, A. C. Garner, P. M. Roberts, A. D. Smith, M. J. Sweet, J. E. Thomson, *Org. Biomol. Chem.* **2006**, *4*, 2753-2768; c) C. G. Barber, D. C. Blakemore, J.-Y. Chiva, R. L. Eastwood, D. S. Middleton, K. A. Paradowski, *Bioorg. Med. Chem. Lett.* **2009**, *19*, 1499-1503.

(56) a) J. W. Hilborn, Z.-H. Lu, A. R. Jurgens, Q. K. Fang, P. Byers, S. A. Wald, C. H. Senanayake, *Tetrahedron Lett.* **2001**, *42*, 8919-8921; b) S. H. Kwak, J. M. Seo, K.-I. Lee, *ARKIVOC* **2010**, 55-61.

(57) a) P. Kumar, R. K. Upadhyay, R. K. Pandey, *Tetrahedron: Asymmetry* **2004**, *15*, 3955-3959; b) G. Wang, X. Liu, G. Zhao, *Tetrahedron: Asymmetry* **2005**, *16*, 1873-1879; c) A. Träff, R. Lihammar, J.-E. Bäckvall, *J. Org. Chem.* **2011**, *76*, 3917-3921; d) A. Kamal, G. B. R. Khanna, R. Ramu, T. Krishnaji, *Tetrahedron Lett.* **2003**, *44*, 4783-4787.

(58) F. A. Cotton, G. Wilkinson, *Inorganic Chemistry. 4th Ed*, **1982**.

(59) C. Bolm, J. Legros, J. Le Paih, L. Zani, *Chem. Rev.* **2004**, *104*, 6217-6254.

(60) a) H. Brunner, R. Eder, B. Hammer, U. Klement, *J. Organomet. Chem.* **1990**, *394*, 555-567; b) H. Brunner, K. Fisch, *Angew. Chem.* **1990**, *102*, 1189-1191; c) H. Brunner, K. Fisch, *J. Organomet. Chem.* **1991**, *412*, C11-C13; d) H. Brunner, M. Roetzer, *J. Organomet. Chem.* **1992**, *425*, 119-124.

(61) a) A. Furuta, H. Nishiyama, *Tetrahedron Lett.* **2007**, *49*, 110-113; b) H. Nishiyama, A. Furuta, *Chem. Commun.* **2007**, 760-762; c) S. Hosokawa, J. Ito, H. Nishiyama, *Organometallics* **2010**, *29*, 5773-5775; d) T. Inagaki, A. Ito, J. Ito, H. Nishiyama, *Angew. Chem., Int. Ed.* **2010**, *49*, 9384-9387; e) T. Inagaki, T. Phong le, A. Furuta, J. Ito, H. Nishiyama, *Chem. Eur. J.* **2010**, *16*, 3090-3096; f) A. Furuta, H. Nishiyama, *Tetrahedron Lett.* **2008**, *49*, 110-113.

(62) a) N. S. Shaikh, K. Junge, M. Beller, *Org. Lett.* **2007**, *9*, 5429-5432; b) N. S. Shaikh, S. Enthaler, K. Junge, M. Beller, *Angew. Chem., Int. Ed.* **2008**, *47*, 2497-2501; c) D. Addis, N. Shaikh, S. Zhou, S. Das, K. Junge, M. Beller, *Chem. Asian J.* **2010**, *5*, 1687-1691.

(63) B. K. Langlotz, H. Wadepohl, L. H. Gade, *Angew. Chem., Int. Ed.* **2008**, *47*, 4670-4674.

(64) a) A. M. Tondreau, E. Lobkovsky, P. J. Chirik, *Org. Lett.* **2008**, *10*, 2789-2792; b) A. M. Tondreau, J. M. Darmon, B. M. Wile, S. K. Floyd, E. Lobkovsky, P. J. Chirik, *Organometallics* **2009**, *28*, 3928-3940.

(65) J. Yang, T. D. Tilley, *Angew. Chem., Int. Ed.* **2010**, *49*, 10186-10188.

(66) S. Diez-Gonzalez, N. Marion, S. P. Nolan, *Chem. Rev.* **2009**, *109*, 3612-3676.

(67) A. J. Arduengo, III, R. L. Harlow, M. Kline, *J. Am. Chem. Soc.* **1991**, *113*, 361-363.

(68) R. W. Alder, P. R. Allen, S. J. Williams, *J. Chem. Soc., Chem. Commun.* **1995**, 1267-1268.

(69) V. V. K. M. Kandepi, J. M. S. Cardoso, E. Peris, B. Royo, *Organometallics* **2010**, *29*, 2777-2782.

(70) P. Buchgraber, L. Toupet, V. Guerchais, *Organometallics* **2003**, *22*, 5144-5147.

(71) a) D. Bezier, G. T. Venkanna, J.-B. Sortais, C. Darcel, *ChemCatChem* **2011**, *3*, 1747-1750; b) F. Jiang, D. Bezier, J.-B. Sortais, C. Darcel, *Adv. Synth. Catal.* **2011**, *353*, 239-244; c) D. Bezier, F. Jiang, T. Roisnel, J.-B. Sortais, C. Darcel, *Eur. J. Inorg. Chem.* **2012**, *2012*, 1333-1337; d) L. C. M. Castro, J.-B. Sortais, C. Darcel, *Chem. Commun.* **2012**, *48*, 151-153.

(72) a) A. Hosomi, H. Hayashida, S. Kohra, Y. Tominaga, *J. Chem. Soc., Chem. Commun.* **1986**, 1411-1412; b) S. Kohra, H. Hayashida, Y. Tominaga, A. Hosomi, *Tetrahedron Lett.* **1988**, *29*, 89-92.
(73) M. Poyatos, A. Maisse-Francois, S. Bellemin-Laponnaz, L. H. Gade, *Organometallics* **2006**, *25*, 2634-2641.
(74) D. J. C. Constable, P. J. Dunn, J. D. Hayler, G. R. Humphrey, J. J. L. Leazer, R. J. Linderman, K. Lorenz, J. Manley, B. A. Pearlman, A. Wells, A. Zaks, T. Y. Zhang, *Green Chem.* **2007**, *9*, 411-420.
(75) R. Kuwano, M. Takahashi, Y. Ito, *Tetrahedron Lett.* **1998**, *39*, 1017-1020.
(76) http://cbc.arizona.edu/njardarson/group/top-pharmaceuticals-poster (Accessed April 2012)
(77) S. Das, B. Join, K. Junge, M. Beller, *Chem. Commun.* **2012**, *48*, 2683-2685.
(78) a) S. Das, D. Addis, K. Junge, M. Beller, *Chem. Eur. J.* **2011**, *17*, 12186-12192; b) S. Das, D. Addis, S. Zhou, K. Junge, M. Beller, *J. Am. Chem. Soc.* **2010**, *132*, 1770-1771.
(79) S. Zhou, K. Junge, D. Addis, S. Das, M. Beller, *Angew. Chem., Int. Ed.* **2009**, *48*, 9507-9510.
(80) Y. Sunada, H. Kawakami, T. Imaoka, Y. Motoyama, H. Nagashima, *Angew. Chem., Int. Ed.* **2009**, *48*, 9511-9514.
(81) H. Tsutsumi, Y. Sunada, H. Nagashima, *Chem. Commun.* **2011**, *47*, 6581-6583.
(82) S. Das, B. Wendt, K. Moeller, K. Junge, M. Beller, *Angew. Chem., Int. Ed.* **2012**, *51*, 1662-1666.
(83) S. L. Buchwald, *Chem. Eng. News* **1993**, *71*, 2.